



HAL
open science

Normal human adipose tissue functions and differentiation in patients with biallelic LPIN1 inactivating mutations

Michele Pelosi, Eric Testet, Soazig Le Lay, Isabelle Dugail, Xiaoyun Tang, Guillaume Mabileau, Yamina Hamel, Marine Madrange, Thomas Blanc, Thierry Odent, et al.

► To cite this version:

Michele Pelosi, Eric Testet, Soazig Le Lay, Isabelle Dugail, Xiaoyun Tang, et al.. Normal human adipose tissue functions and differentiation in patients with biallelic LPIN1 inactivating mutations. *Journal of Lipid Research*, 2017, 58 (12), pp.2348-2364. 10.1194/jlr.P075440 . hal-02521228

HAL Id: hal-02521228

<https://univ-angers.hal.science/hal-02521228>

Submitted on 27 Mar 2020

HAL is a multi-disciplinary open access archive for the deposit and dissemination of scientific research documents, whether they are published or not. The documents may come from teaching and research institutions in France or abroad, or from public or private research centers.

L'archive ouverte pluridisciplinaire **HAL**, est destinée au dépôt et à la diffusion de documents scientifiques de niveau recherche, publiés ou non, émanant des établissements d'enseignement et de recherche français ou étrangers, des laboratoires publics ou privés.



Distributed under a Creative Commons Attribution 4.0 International License

Normal human adipose tissue functions and differentiation in patients with biallelic *LPIN1* inactivating mutations.

Michele Pelosi*(1), Eric Testet (2), Soazig Le Lay (3), Isabelle Dugail (4), Xiaoyun Tang (5), Guillaume Mabileau (6), Yamina Hamel (1), Marine Madrange (1), Thomas Blanc (7), Thierry Odent (8), Todd P.W. McMullen (9), Marco Alfò (10), David N. Brindley (5), Pascale de Lonlay*(1).

*M. Pelosi and P. de Lonlay: co-corresponding Authors.

(1) Centre de Référence des Maladies Héritaires du Métabolisme, Institut Imagine des Maladies Génétiques, Laboratoire de génétique des maladies autoinflammatoires monogéniques, INSERM UMR1163, Université Paris Descartes et Hôpital Necker-Enfants malades (Assistance publique – Hôpitaux de Paris), Paris, France.

(2) Laboratoire de Biogenèse Membranaire-UMR 5200, CNRS, Université de Bordeaux, Villenave d'Ornon, France.

(3) INSERM, UMR1063, Université d'Angers, UBL, Angers, France.

(4) INSERM, U1166, Equipe 6, Université Pierre et Marie Curie, Paris, France.

(5) Department of Biochemistry, Signal Transduction Research Group, University of Alberta, Edmonton, Alberta, T6G 2S2, Canada.

(6) SCIAM, Université d'Angers, Angers, France.

(7) Department of Pediatric Surgery and Urology, Necker Enfants-Malades Hospital-Université Paris Descartes, Sorbonne Paris Cite, Paris, France.

(8) Department of Pediatric Orthopaedics, Necker Enfants-Malades Hospital-Université Paris Descartes, Sorbonne Paris Cite, Paris, France.

(9) Department of Surgery, University of Alberta, Edmonton, Alberta, T6G 2R7, Canada.

(10) Dipartimento di Scienze Statistiche, Sapienza Università di Roma, Rome, Italy.

CONTACT INFORMATION FOR CORRESPONDING AUTHORS:

Pascale de Lonlay and Michele Pelosi, co-corresponding authors, c/o INSERM UMR1163, Institut Imagine des Maladies Génétiques, Université Paris Descartes et Centre de Référence des Maladies Héritaires du Métabolisme, Hôpital Necker, AP- AP-HP, Paris, France. E-mail: pdelonlay@neuf.fr ; michi_pelo@libero.it .

Mail Address: Institut Imagine, 24 Bd Montparnasse, 75015 Paris, telephone 00 33 1 44 49 40 23,

fax number 00 33 1 44 49 48 50, E-mail address: pdelonlay@neuf.fr; michi_pelo@libero.it .

RUNNING TITLE: Adipose tissue functions in patients with *LPIN1* mutations.

ABBREVIATIONS: PAP: phosphatidic acid phosphatase; TAG: triacylglycerols; PL: polar lipids; PA: phosphatidate; WAT: white adipose tissue; FAO: fatty acids oxidation; TLC: thin layer chromatography; LD: lipid droplets; FA: unesterified fatty acids; GC-FID: gas chromatography-flame ionization detector; LCFA: long-chain fatty acids; HDF: human dermal fibroblasts; GM: growth medium; DM: differentiation medium; DXM: dexamethasone; IBMX: isobutylmethylxanthine; MSC: mesenchymal stem cells; SREBP1: Sterol regulatory element-binding protein 1; PPAR: Peroxisome proliferator-activated receptors; PGC1A: Peroxisome proliferator-activated receptor gamma coactivator 1-alpha; NFATc4: Nuclear factor of activated T-cells, cytoplasmic 4; VCAM-1: vascular cell adhesion molecule 1 (or cluster of differentiation 106, CD106); MCAM: melanoma cell adhesion molecule (or cluster of differentiation 146, CD146); ITGA11: integrin alpha-11; MME: neprilysin or membrane metallo-endopeptidase (or cluster of differentiation 10, CD10); DPP4: dipeptidyl peptidase-4 (or cluster of differentiation 26, CD26); FASN: fatty acid synthase; LPP: lipid phosphate phosphatase; SGBS: Simpson-Golabi-Behmel syndrome.

ABSTRACT

Lipin-1 is a Mg^{2+} -dependent phosphatidic acid phosphatase (PAP) that in mice is necessary for normal glycerolipid biosynthesis, controlling adipocytes metabolism and adipogenic differentiation. Mice carrying inactivating mutations in the *Lpin1* gene display the characteristic features of human familial lipodystrophy. Very little is known on the roles of lipin-1 in human adipocyte physiology. Apparently fat distribution and weight is normal in humans carrying *LPINI* inactivating mutations, but a detailed analysis of adipose tissue appearance and functions in these patients has not been available so far. In this study, we performed a systematic histopathological, biochemical and gene expression analysis of adipose tissue biopsies from human patients harbouring *LPINI* biallelic inactivating mutations and affected by recurrent episodes of severe rhabdomyolysis. We also explored the adipogenic differentiation potential of human mesenchymal cell populations derived from lipin-1 defective patients. White adipose tissue from human *LPINI* mutant patients displayed a dramatic decrease in lipin-1 protein levels and PAP activity, with a concomitant moderate reduction of the adipocyte size. Nevertheless the adipose tissue develops without obvious histological signs of lipodystrophy and with a normal qualitative composition of the storage lipids. The increased expression of key adipogenic determinants such as *SREBP1*, *PPARG* and *PGC1A* shows that specific compensatory phenomena can be activated in vivo in human adipocytes under deficiency of a functional lipin-1.

Keywords:

Adipocytes, Adipose tissue, Gene expression, Lipodystrophies, Phosphatases/Lipid, Inborn errors of metabolism, Human lipids, Lipin-1, Adipogenic differentiation, Human fat lipid analysis.

INTRODUCTION

Studies in vitro and in vivo using mouse models showed that the protein lipin-1, encoded by the gene *Lpin1*, is an enzyme necessary for normal glycerolipid biosynthesis, which is also able to control the adipocyte metabolism and adipogenic differentiation (1-7). Lipin proteins act as Mg^{2+} -dependent phosphatidate phosphatases (PAP) that catalyze the dephosphorylation of phosphatidate (PA) to diacylglycerol (DAG), a direct precursor of triacylglycerols (TAG) and polar lipids (PL), such as phosphatidylethanolamine (PE) and phosphatidylcholine (PC) (8-10). Although lipin-1 does not have a DNA-binding motif, it is able to translocate to the nucleus of hepatocytes and adipocytes, where it can act as a transcriptional co-regulator (3, 11-14), interacting with $PGC1\alpha/PPAR\alpha$ and $PPAR\gamma$, modulating their transcriptional activity and regulating adipogenesis, fatty acids oxidation (FAO) and the expression of key components of the mitochondrial respiratory chain (11-13, 15). Accordingly, lipin-1 deficient mice exhibit reduced expression of hepatic PPAR-regulated genes and impaired FAO activity (13, 16, 17). The effects of lipin-1 on transcription do not apparently require lipin-1 PAP activity, demonstrating that the enzymatic activity of lipin-1 can be functionally separated from its ability to co-regulate the transcription (11-13, 18). Moreover, lipin-1 has also been implicated in the modulation of pro-inflammatory responses both repressing NFATc4 activity and downstream cytokine production in the adipocytes (15) and positively controlling the production of pro-inflammatory factors during macrophage activation (19, 20).

Lpin1 fatty liver dystrophic (fld) mice, i.e. *Lpin1*^(fld/fld) deficient mice, carrying spontaneous inactivating mutations in the *Lpin1* gene, show the characteristic features of the human congenital lipodystrophy (1-3, 7). This condition consists of a group of genetic disorders characterized by severe loss of body fat, associated with metabolic disturbances such as fatty liver, hypertriglyceridemia and insulin resistance (21). The absence or decreased levels of PAP activity in the white adipose tissue (WAT) of the *Lpin1*^(fld/fld) mice as well in the WAT of other mouse or rat models without a functional lipin-1, result in dysregulated TAG biosynthesis, with the subsequent accumulation of PA (2, 5, 7, 14, 16, 22-25). The lipodystrophic lipin-1-deficient mouse models are characterized by: i) an impaired maintenance of the mature adipocytes, with a severe reduction in TAG storage and a consequent severe reduction (about 80%) of the fat body mass; ii) the presence of abnormal adipocytes,

with multilocular lipid droplets; iii) an impairment in adipogenic differentiation, with an important increase in the presence of immature adipocytes in the WAT (5, 7, 14). The rat model with a dominant negative mutation in the *Lpin1* gene (the *Lpin1*^{LHubr} rats) presents a milder but analogous form of lipodystrophy, characterized by impaired expression of key transcriptional adipogenic factors such as PGC1 α and PPAR α (24). Unexpectedly, the *Lpin1*^(fld/fld) mouse does not show defects in TAG synthesis or β -oxidation in the heart where lipin-1 provides about 80% of the PAP activity and in this case the presence of the paralogues lipin-2 or lipin-3 appears to compensate for the absence of lipin-1 (25).

The accumulated evidence from observations in lipin-1 deficient rodents models presents a lipodystrophic phenotype, together with data showing that lipin-1 is involved in the adipogenesis in vitro (3, 4, 6, 26). The observations that the gene encoding for lipin-1 is prevalently expressed in adipose tissue in human beings and mouse (9), make *LPINI* a top-rank candidate for human lipodystrophy. However, we and other investigators have reported that the presence of *LPINI* inactivating mutations in human patients leads to a dramatic and peculiar skeletal muscle-related pathological phenotype, which consists of recurrent and severe episodes of rhabdomyolysis (i.e. massive breakdown of the skeletal muscle fibers), without any evident involvement of the adipose tissue (27-29). Consistent with the prevailing human phenotype, the absence of lipin-1 can induce a failure in the maintenance of muscle integrity under special conditions of metabolic stress in *Lpin1*^(fld/fld) mice (30).

The role of lipins in human adipogenesis and human adipose tissue functions is still undefined. Recently it was shown in human Simpson-Golabi-Behmel syndrome (SGBS) pre-adipocyte cell line (an in vitro cell model for studies of human adipocyte differentiation) that lipin-1 is progressively induced during adipogenesis and that depletion of lipin-1 by siRNA, leads to depletion of about 95% of the PAP activity and to a significant reduction of the key adipogenic transcription factors PPARG and SREBP1 (31). Nevertheless, the SGBS cell line differentiated normally and accumulated neutral lipids under deficiency of lipin-1, supporting the hypothesis of the existence of alternative pathways for TAG synthesis in human adipocytes subjected to conditions of repressed lipin-1 expression (31).

In-depth biochemical, histological and biological analyses of adipose tissue derived from lipin-1 defective patients have not been performed so far. In spite of the absence of obvious signs of adipose tissue loss and lack of the metabolic disturbances usually associated with lipodystrophy, we cannot yet exclude that human lipin-1 defective individuals (as in rodents) manifest some failures of adipose tissue homeostasis. To clarify the effects of lipin-1 deficiency on human adipose tissue, we performed a systematic analysis of WAT biopsies derived from patients carrying biallelic *LPINI* inactivating mutations. Also, to assess the possible role played by lipin-1 in human adipogenesis, we triggered the adipogenic differentiation potential of primary mesenchymal cells derived from lipin-1 defective patients.

Our analysis established that the adipose tissue from human lipin-1 defective patients is characterized by a marked decrease in lipin-1 protein levels and PAP activity, with a concomitant moderate reduction of the adipocyte size. However, WAT in lipin-1 defective human individuals develops without detectable histopathological signs of lipodystrophy and with an apparently normal qualitative composition of stored lipids. The increased expression of key adipogenic determinants such as *SREBP1*, *PPARG* and *PGC1A* shows that a specific compensatory phenomenon can be activated in vivo in human adipocytes in the presence of depleted lipin-1 expression.

MATERIALS and METHODS

Materials. All reagents were purchased from Sigma-Aldrich, unless otherwise specified.

Patients and healthy control individuals. All the patients were clinically and genetically characterized, and they suffered from recurrent episodes of rhabdomyolysis (27, 28, 29, 32). When fat biopsies were taken, the patients were apparently in good health, fully compensated, and not suffering of episodes of rhabdomyolysis for several months. Table 1 summarizes the characterization of the patients and healthy control individuals used in the present study.

Biopsy method. Subcutaneous WAT samples biopsies were obtained from the brachial region (deltoid region) of the lipin-1 defective patients, or from the dorsal region for the control individuals. Only in Fig. 4 two WAT control biopsies were from breast adipose tissue from healthy adult individuals (aged 53 and 56) subjected to reduction mastoplasty. Otherwise, the collection of the WAT samples required a <0.5 cm scalpel incision, and subsequent collection of the biopsy, using a 14-Gauge needle. Adipose tissue samples were rapidly rinsed in PBS and immediately analysed or frozen. This work has been approved by the Hôpital Necker-Enfant Malades Ethical Committee after declaration to the *Département de la Recherche Clinique et du Développement* (Assistance Publique, Hôpitaux de Paris, France) and informed consent was provided (by a parent or guardian for each child). Breast adipose tissue (controls B1 and B2 in Fig. 4) was obtained with approval of the University of Alberta Health Research Ethics Board ID Pro00018758, with written informed consent.

Electron microscopy. WAT biopsies (~8 mm³) were fixed for 16 h at 4°C in 2.5% glutaraldehyde in 0.1 M Sorensen's buffer, pH 7.4. Samples were rinsed in 0.2 M cacodylate buffer, pH 7.4, and subsequently post-fixed with 2% osmium tetroxide/1.5% potassium ferrocyanide in 0.2 M cacodylate buffer, pH 7.4, for 45 min at room temperature. Samples were then rinsed with distilled water, dehydrated in ethanol and embedded in EMbed 812 epoxy resin (LFG Distribution) at 60°C for 48 h. Semi-thin sections (1 µm-thickness) were cut with an EM-UC7

ultramicrotome (Leica), colored with 1% methylene blue/1% Azur B and observed with an Olympus AX-60 microscope (Olympus) equipped with a QImaging QIClick digital CCD camera (QImaging, Surrey, BC, Canada). Thin sections (60 nm-thickness) were cut and counterstained with uranyl acetate and observed with a Jeol JEM 1400 microscope (Jeol, Croissy sur Seine, France) operated at 120 KeV and equipped with a Gatan Orius Camera (Gatan, Pleasanton, CA, USA).

Immunohistofluorescence. Adipose tissue biopsies (WAT) were fixed for 12-16 h at room temperature in 4% paraformaldehyde and embedded in paraffin. Five μm sections were cut at 50 μm intervals and mounted on charged glass slides. Paraffin was removed with xylene, and slides were stained for the expression of perilipin, using an anti-perilipin-1/PLIN1 antibody (Progen) as described (33). Adipose tissue sections were stained with DAPI, prior to mounting them using the mounting medium Fluoromount-G (SouthernBiotech). The total numbers of nuclei and adipocytes were counted in 5 microscopic fields for each biopsy. The adipose tissue cellular composition was then determined for each histological sample as the total number of adipocytes (in which perilipin-1 decorates an unilocular lipid droplet, occupying the entire cell volume) divided by the total number of nuclei (DAPI positive).

Adipocytes diameter measurements. Fat biopsies ($\sim 8 \text{ mm}^3$) were fixed as indicated in the “Electron Microscopy” section (see above); semi-thin sections (500 nm-thickness) were cut with an EM-UC7 ultramicrotome (Leica), colored with 1% methylene blue/1% Azur B and observed with an AX-60 microscope as indicated above. Adipocyte diameters (expressed in μm) of at least 100 mature adipocytes in each section were measured on microscopic images, using Image J software. The cumulative distribution function (CDF) of the adipocytes diameters was estimated statistically by the empirical cumulative function (ECDF) (see Fig. 3). The measured adipocytes diameters for each experimental individual or group were divided into arbitrary classes, with $\sim 16 \mu\text{m}$ intervals. The Kolmogorov-Smirnov test was used as a non-parametric statistic to test the equality of CDFs, i.e. testing the null hypothesis that the samples were drawn from the same population (described by the

corresponding CDF). All statistical analyses, including graphical representations and exploratory statistics, were performed using the open source software R, release 3.2.2 “Fire safety” (34).

Enzymatic activity for PAP. An enzymatic assay for PAP was performed as described in (25). Briefly, adipose tissue was homogenized in sucrose buffer consisting of 250 mM sucrose, 0.6 mM dithiothreitol (DTT) and protease inhibitor cocktail, followed by centrifugation to collect the infranatant in which PAP activity was measured. Each sample was assayed in a total volume of 100 μ l consisting of 100 mM Tris/HCl (pH 7.4) containing 0.6 mM DTT, 1.5 mM $MgCl_2$, 2 mg/ml fat-free BSA, protease inhibitor cocktail, 30 nM microcystin-LR, 0.6 mM phosphatidate (PA) labelled with [3H]palmitate {[9,10- $^3H(N)$]-palmitic Acid, PerkinElmer}, 1 mM EDTA/EGTA, 0.4 mM phosphatidylcholine, and 200 μ M tetrahydrolipstatin to block lipase activity. Parallel measurements were performed in the absence of Mg^{2+} and in the presence of 8 mM N-ethylmaleimide (NEM) to determine the contribution from lipid phosphate phosphatase (LPP) activity. The diacylglycerol that was formed was extracted in 2 ml of chloroform-methanol (19:5, v/v) containing 0.08% olive oil as carrier. Activated alumina was added to remove the unreacted PA and any liberated [3H]palmitate from the chloroform phase. The chloroform phase was dried, and the radioactivity determined. PAP activity was calculated by subtracting the NEM-insensitive LPP activity from the total phosphatidate phosphatase activity. Each sample was assayed at three different protein concentrations to ensure a proportional response.

Western blotting analysis for lipin-1. Adipose tissue was homogenized in RIPA buffer followed by centrifugation. The infranatant was collected and four volumes of ice-cold acetone were added to precipitate protein. After centrifugation at 12,000xg for 10 min, protein precipitations were washed with one volume of ice-cold acetone and proteins were dried at room temperature. Protein precipitations were resuspended in RIPA buffer. Sixty μ g of protein was loaded for PAGE (25) and probed with anti-lipin1/LPIN1 antibody (Abcam) or with an anti tubulin antibody as a loading control. Blots were analyzed by Li-cor C-DiGit Blot imaging scanner.

Lipid analysis. WAT (about 15-20 mm³) were extracted in 2 ml of chloroform/methanol 2:1, (v/v) using a glass Potter-Elvehjem homogenizer with a PTFE pestle. 500 µl of 1% perchloric acid was added and the extracted suspension vortexed for 30 s. After centrifugation, the organic phase was isolated, and the aqueous phase further extracted with 2 ml of chloroform/methanol 2:1 (v/v). The two organic phases were pooled in a glass test tube (test tube A) and evaporated to dryness. A fully quantitative procedure to efficiently separate the less abundant total PL from the highly prevalent TAG from total lipid extracts from each fat biopsy was adapted from a previously described two-phase hexane/(ethanol-water) extraction method (35). Briefly, a stock biphasic solvent system was prepared by mixing equal volumes of hexane and an aqueous ethanol solution (13% water, 87% ethanol, by vol.). 4.5 ml of the upper phase and 1.5 ml of the lower phase of the biphasic solvent system were added to the test tube A, containing the dried extracted lipids, and mixed thoroughly. The extracted lower phase from the test tube A was transferred to a second test tube (B) containing 4.5 ml of pre-equilibrated upper phase stock solvent system. 1.5 ml of the lower phase of the stock solvent system was added to the test tube A. Test tubes A and B were mixed thoroughly and after equilibration the lower phase of the test tube B was isolated, and the lower phase of the test tube A was transferred to the test tube B. The above procedure was repeated six times. The combined upper phases (i.e. 8 times 1.5 ml) represented the ethanolic phase, prevalently containing PL (Fig. 3), and the remaining upper phases from test tube A and B represented the hexane phase #1 and the hexane phase #2, respectively, prevalently containing neutral lipids (Fig. 3). The different extracted phases were evaporated to dryness and re-dissolved in 4 ml (for the hexane phase #1) or 100 µl (for the hexane phase #2 and the ethanolic phase) of chloroform/methanol (2:1, v/v). 100 µl of the hexane phases and of the ethanolic phase were analyzed by one-dimensional high performance TLC on silica gel 60 (Merck) using hexane/diethyl ether/acetic acid (90:15:2, v/v/v) as mobile phase for neutral lipid separation (36, 37) and using chloroform, methanol, water, ammonia 25% (60:34:4:2, v/v/v/v) as mobile phase for the polar lipid separation (38). The lipids were then located by spraying the TLC plates with 0.001% (w/v) primuline in 80% acetone, followed by Imaging (ChemiDoc, Bio-Rad).

The silica gel zones corresponding to TAG and PL were scrapped from the TLC plates and the acyl chains analyzed by gas-chromatography (GC-FID). The spot scrapped were added to 1 ml of methanol/2.5%

H₂SO₄ containing 5 μg of heptadecanoic acid methyl ester. After maintaining the lipids in the mixture at 80°C for 1 h, 1.5 ml of water was added and FA methyl esters extracted using 0.75 ml of hexane. Separation of FA methylesters was performed by GC (Hewlett–Packard 5890, series II) on a 15 m×0.53 mm Carbowax column (Alltech Associates, Deerfield, IL) by flame-ionization detection (GC-FID). The retention times of FA methylesters were determined by comparison with standards, and they were quantified using heptadecanoic acid methyl ester as a standard (39).

Isolation of dermal fibroblasts. Human primary dermal fibroblasts populations were established from biopsy specimens obtained from the brachial region (deltoid region) of lipin-1 defective patients or from the dorsal forearm region for the controls individuals. Tissue biopsies were dissociated enzymatically in 0.25% collagenase type I and 0.05% DNase in DMEM with 20% foetal bovine serum (FBS) overnight, at 37°C. Primary fibroblast cultures were established in 25-cm² culture flasks in DMEM, supplemented with 20% fetal calf serum (FCS) and 2 mM glutamine. Monolayer cultures were maintained at 37°C in 10% CO₂ until about 70% confluence. Cells were then passaged and used for experiments.

Adipogenic differentiation of human primary dermal fibroblasts populations. Human primary dermal fibroblasts were plated in Growth Medium (GM) containing DMEM + 2 mM glutamine and 10% FCS (all from Life Technologies), on culture dishes. After two days of post-confluence (which was considered as day 0), cells were shifted in adipogenic differentiation medium (DM) containing DMEM + 2 mM glutamine, 10% FCS, 500 nM bovine insulin, 500 nM dexamethasone, 500 μM 3-Isobutyl-1-methylxanthine and 50 μM indomethacin or in control medium (DMEM + 2 mM glutamine, containing 10% FCS). Every two days the DM or the control medium was replaced, and at 4, 8 and 12 days cells were collected for the RNA extraction and for further analysis.

RNA isolation, RT (reverse transcription) and real time PCR. Human primary dermal fibroblasts cells were washed with ice-cold PBS and total RNA was extracted using the TRIzol reagent (Life Technologies). Human

fat biopsies (WAT, about 5-10 mm³) were rinsed in cold PBS and immediately frozen in liquid nitrogen; subsequently biopsies were homogenized in about 500 ml of TRIzol Reagent using a glass Potter-Elvehjem homogenizer with a glass pestle. The homogenate was subjected to centrifugation at 12,000xg for 8 min at 4°C. The pellet and the top fat layer were discarded whereas the aqueous phase was subjected to standard TRIzol protocol according to manufacturer's instructions, for total RNA purification. Digestion of contaminating genomic DNA was performed with DNA-free DNase treatment (Ambion). First strand cDNA was generated using a kit with random primers (High Capacity cDNA Reverse Transcription kit, Applied Biosystems) from 1 µg of total RNA. Newly synthesized cDNA was diluted 5-fold in DNase-free water, and 5% of this cDNA was used in each real-time PCR assay, using a 7500 Real Time PCR System (Applied Biosystems) (40, 41). The standard curve method was used to calculate the relative mRNA levels for each transcript examined and human was used as a reference to normalize the results. The sequence (5' to 3') of the specific primers used for the SYBR Green quantification of the mRNA (Power SYBR Green PCR Master Mix, Applied Biosystems) were: MME, human membrane metallo-endopeptidase: forward primer: CCTCACCATCATAGCTGTGACAA; reverse primer: TGA CTTGCAAATACCATCATCGT. MCAM, human melanoma cell adhesion molecule: forward primer: CCTGGACTTGGACACCATGAT; reverse primer: ACGTCAGACACATAGTTCACCAGTAGT. VCAM1, human vascular cell adhesion molecule 1: forward primer: CAAAGGCAGAGTACGCAAACAC; reverse primer: GCTGACCAAGACGGTTGTATCTC. ITGA11, human integrin alpha 11: forward primer: GCACCCCATTTCCAAACAAC; reverse primer: ACCGCCTCTCATCCATGGT. DPP4, human dipeptidyl-peptidase 4: forward primer: CAGTCACCAATGCAACTTCCA; reverse primer: ACAAGTAGTGATCCCCTATCAACATAGA. PPAR-γ, human peroxisome proliferator-activated receptor gamma (PPARG): forward primer: GGGCGATCTTGACAGGAAAG; reverse primer: CCCATCATTAAGGAATTCATGTCAT. FASN, human fatty acid synthase: forward primer: CAGACGAGAGCACCTTTGATGAC; reverse primer: CAGGTCTATGAGGCCTATCTGGAT. PGC1-α, human peroxisome proliferator-activated receptor gamma, coactivator 1 alpha (PPARGC1A): forward primer: ACCCAGAACCATGCAAATCAC; reverse primer: GCTCCATGAATTCTCAGTCTTAACAA. LPIN1, human lipin-1: forward primer: TGAAAAGGGGCTCTGTGGAC; reverse primer: ACTACAGAGCTGCTTGACGG. LPIN2, human Lipin-2: forward primer:

GGTCCCCTTTAGAGACCACCTATC; reverse primer: CACCTCCAGCTCTGAATCACTCTT. ACTB, human actin beta: forward primer: CTGGCACCCAGCACAATG; reverse primer: CCGATCCACACGGAGTACTTG. SREBF1, human sterol regulatory element binding transcription factor 1: forward primer: GCTGTCCACAAAAGCAAATCTCT; reverse primer: TCAGTGTGTCCTCCACCTCAGT.

RESULTS

Histomorphometrical and ultrastructural analyses of human adipose tissue in patients carrying biallelic *LPIN1* mutations.

Mice carrying inactivating mutations of the *Lpin1* gene are characterized by manifested lipodystrophy features, with a severe reduction of total fat mass, presence of abnormal adipocytes with multilocular lipid droplets and a significant increase of immature adipocytes in the adipose tissue (2, 7, 14). The role of lipins in human adipogenesis is still undefined. To investigate the consequences of the deficiency of lipin-1 in human adipogenesis, we examined fat biopsies from human patients carrying biallelic inactivating mutations in the *LPIN1* gene, to search for signs of defects in the histological structure, indicative of lipodystrophy.

According to previous studies, two divergent histopathological subsets can be observed in congenital or acquired forms of human lipodystrophy (42). One form of lipodystrophy is characterized histologically: i) by small adipocytes, embedded in hyaline connective tissue, ii) by the presence of a myxoid stroma with numerous capillaries, and iii) by a very scarce infiltration of inflammatory cells (42). The second type of human lipodystrophy is characterized instead by a distinctive "inflammation of the fat", with the hallmark presence of focal lymphocytes, histiocytes and plasma cells, but showing normal-appearing adipocytes and normal vasculature (42). In all cases lipodystrophic adipose tissue can be recognized histologically by alteration in the proportions of mature fat cells to non-fat cells (33).

Mature adipocytes (and the shape of the lipid droplets) were identified on histological adipose tissues sections, based on their characteristic perilipin-staining of the monolocular lipid droplet ((43) and Fig. 2). Perilipin-1 was abundantly expressed in mature adipocytes, where it localized at the surface of the intracellular lipids droplets (LD) (43). Like in the normal controls, the histological and ultrastructural analyses of the human fat biopsies from lipin-1 defective patients did not show any evidence of histopathological features associated with lipodystrophy (Fig. 1 and 2). No manifest signs suggestive of hypoplastic development, inflammation, increased presence of stromal cells or perturbation of the morphology (i.e. increased presence of mixoid stroma, lobules of small adipocytes, or abnormal vasculature) were observed by histological and ultrastructural analyses of the adipose tissue from lipin-1 defective patients (Fig. 1 and 2).

We did not observe abnormal or multilocular lipid droplets (Fig. 2). Perilipin immunostaining of the lipid droplets was conserved, since it decorated unilocular LD occupying the entire cell volume of the adipocytes (Fig. 2). The ultrastructural analysis confirmed the full integrity of the LD membrane and structure in lipin-1 defective patients (Fig. 1 C and F).

We next assessed the ratio between the number of mature adipocytes (showing large perilipin-1-positive monolocular LD) and the number of cells (based on DAPI nuclei detection) in adipose tissue histological sections (Fig. 2). This enabled us to detect possible changes in the proportion between adipocyte and non-adipocyte cells (including the stromal cells fraction). Significant decreased values in this ratio are indicative of adipose tissue infiltration by non-adipose cells, disclosing an inflammatory state or suggesting an hypoplastic development of the adipose tissue, which are often observed in lipodystrophies (33). The ratio perilipin/DAPI was not significantly affected in human adipose tissue from patients carrying biallelic *LPIN1* inactivating mutations compared to normal control individuals (Fig. 2). This result indicates that adipose tissue from lipin-1 defective patients was not significantly hypoplastic or infiltrated with immature adipocytes and non-adipocytic cells, including inflammatory cells.

Some forms of mild lipodystrophy are characterized by the presence of adipocytes with a reduced size (42), and this feature is symptomatic of a deficiency in accumulation of TAG in the LDs. We performed a semiautomated histomorphometric analysis of the diameter of the adipocytes in fat biopsies from normal controls and from patients harbouring *LPIN1* inactivating mutations.

At first we proceeded to calculate exploratory statistics for the diameter of the adipocytes for the entire groups of controls and patients, suggesting a possible decrease in adipocyte diameter in patients when compared to the controls (Table 2 A). Subsequently, individual histogram representations of the adipocyte diameter distribution were built for both controls and patients, considering each individual separately (Fig. 3 A). Analogously, histograms of the adipocytes diameter distribution were also built for the entire group of the controls and the entire group of the patients (Fig. 3 B).

The empirical cumulative distribution function (ECDF) of the adipocytes diameter was then calculated for the grouped controls versus the grouped patients (Fig. 3 C). The adipocyte size for the grouped patients (n=4) was significantly smaller compared to grouped normal controls (n=5), as statistically tested by the Kolmogorov-Smirnov non-parametric test (KS-test) (Table 2 B and Fig. 3 C).

To minimize possible confounding effects of age on the adipocyte size, we also adopted a special statistical analysis: the ECDF of the adipocytes diameters were calculated for each patient and for the grouped controls, and the KS-test was applied to test the null hypothesis that the values observed on each patient were drawn from the same CDF of the grouped controls (see Table 2 B). Adipocyte sizes for three out of four patients studied (i.e., for patient 1, age 5; for patient 3, age 11; and for patient 4, age 47) were significantly smaller compared to grouped normal controls (see Table 2 B and Fig. 3 A).

In conclusion, no significant signs of perturbation of the morphology, hypoplastic development or inflammation were observed in adipose tissue of patients carrying *LPINI* inactivating mutations. We found a significant (albeit moderate) reduction in adipocyte size. This latter observation indicates a slightly decreased capacity of fat accumulation in the LDs in the adipose tissue of patients harbouring biallelic *LPINI* mutations. However, we cannot exclude the possibility that the reduced adipocyte size might also depend on confounding factors, which are not fully controllable under our experimental conditions.

Analysis of lipin expression levels and PAP activity in the adipose tissue of patients carrying biallelic *LPINI* mutations.

We also analysed the *LPINI* gene expression levels, the lipin-1 protein levels, and PAP activity in fat biopsies from human patients carrying *LPINI* biallelic inactivating mutations. The *LPINI* deleterious mutations lead to stop codons or internal deletions (see Table 1 and (27-29, 32)). Real-time PCR analysis showed significantly lower *LPINI* mRNA levels in the adipose tissue from patients compared with normal controls (Fig. 6 D). This could depend on an intracellular instability of the mutated/truncated *LPINI* mRNA variants, which could be more rapidly degraded, compared to non-mutated (WT) *LPINI* mRNA (44).

WAT from patients carrying *LPINI* homozygous early stop mutations (p.Arg388X/p.Arg388X) or heterozygous *LPINI* mutations (p.Asn417LysfsX22/p.Glu766_Ser838del, i.e. an early stop mutation and a C-terminal deletion), showed dramatically reduced the levels of lipin-1, without significant differences in lipin-1 expression between homozygous and heterozygous mutant alleles (Fig. 4 A and B). This suggests that mRNA resulting from the *LPINI* 3'-terminal deletion mutant alleles in the heterozygous patients is unstable. (29).

However, in none of the patients analysed was the apparent expression of lipin-1 completely abolished: a weak protein band of about 100 kDa was still recognized in both types of *LPINI* biallelic inactivating mutations (Fig. 4 A). On average, ~23% of the staining was still present in WB of WAT from patients carrying *LPINI* mutations (Fig. 4 A and B). We hypothesize that it could correspond to lipin-2 since the anti-human lipin-1 antibody that we used in the WB analysis can also weakly cross-react with the 98 kDa lipin-2 (results not shown).

All patients showed a similar dramatic impairment of PAP activity in their WAT with only ~13% of the PAP activity of the controls (Fig. 4 C). There were no significant differences in PAP activity between the homozygous and compound heterozygous alleles. This result shows that lipin-1 accounts for the majority PAP activity in human WAT, as expected. We also obtained previous evidence in primary myoblasts established from lipin-1 defective patients (29), that different *LPINI* mutant alleles (homozygous C-terminal deletion, homozygous early stop mutation, and heterozygous early stop mutation + C-terminal deletion) are all associated with a severe reduction of PAP activity, although this was not totally abolished (29).

We hypothesized that lipin-2 and lipin-3 can contribute to the residual PAP activity in lipin-1 defective patients (9, 45). Therefore, we explored the possibility of a compensatory overexpression of *LPIN2* or *LPIN3* in human adipose tissue in presence of deleterious mutation of *LPINI* (9, 45). *LPIN2* mRNA expression levels were not significantly modulated in lipin-1 defective patients compared to controls (Fig. 6 E). Moreover, *LPIN3* mRNA was always undetectable by real-time PCR in the adipose tissue biopsies of both patients and controls (results not shown). This is consistent with previous observations, showing that *LPIN3* is selectively expressed in intestine, platelets, B-lymphocytes, and in a subset of neuronal cells, but virtually absent in other tissues, like adipose and muscle (Ref. (9) and see the BioGPS gene annotation web portal (46)).

Altogether these results suggest that: i) lipin-1 defective patients had severely reduced *LPIN1*/lipin-1 expression and PAP activity; ii) lipin-1 accounts for the majority PAP activity in human WAT; iii) the expression of *LPIN2* potentially appears to provide the residual PAP activity in lipin-1-deficient patients; and iv) there appeared to be no compensatory mechanisms that increase the expression of *LPIN2* or *LPIN3*.

Qualitative analysis of lipids in human adipose tissue from lipin-1 defective patients.

To further understand the functions of lipin-1 in human adipose tissue, we explored the qualitative composition of the storage lipids in human WAT biopsies from lipin-1 defective patients.

A quantitative (i.e. absolute) determination of the lipid content in the adipose tissue biopsies was difficult, due to lack of tissue homogeneity among different biopsies. In fact, each minute biopsied adipose sample was characterized by a variable and uncontrollable intrinsic presence of stromal, connective and vascular tissues, which makes normalization based on the mass of protein or the total mass of each biopsy impractical. A rigorous compromise in our analysis was to quantify the relative abundance of TAG and PL in the total lipid extracts from each biopsy (Fig. 5 E and (39)).

We applied a fully quantitative procedure to separate total PL and TAG from total lipid extracts derived from each fat biopsy (35). Representative TLCs for the extracted lipid fractions are shown for a patient and a control individual in Fig. 5 A-D.

Our qualitative analysis of the lipids in human WAT showed that: i) inactivating mutations in the *LPIN1* gene which severely compromise the PAP activity, do not significantly affect the relative proportions between TAG and PL, compared to normal controls (Fig. 5 E), and do not apparently affect the general qualitative lipid landscape, as shown by TLC analysis (Fig. 5 A-D). ii) as a general physiological observation, the $LCFA_{TAG}$ exceed, on average, about 2,000 times the $LCFA_{PL}$ (Fig. 5 E), and the ratio $LCFA_{TAG}/LCFA_{PL}$ offers a clear estimate of the prevalence of TAG over PL in human WAT. iii) storage lipids from lipin-1 defective patients do not show abnormal accumulation of unesterified FA (Fig. 5 A-D). iv) in TAG extracts from lipin-1 defective patients, the impairment of lipin-1 does not significantly affect the relative abundance of unsaturated and saturated long chain fatty acids ($LCFA_{TAG}$ 16:0, 16:1, 18:0, 18:1 and 18:2), compared to normal control

individuals (see analysis in Table 3).

As mentioned before, the absence or decreased levels of PAP activity in the WAT in mouse or rat models without a functional lipin-1, results in dysregulated TAG biosynthesis, with the subsequent accumulation of PA (2, 16, 23, 24). Because the very limited amount of the starting WAT biopsies, and the intrinsic low levels of PA, using an enzymatic method (47) or direct TLC methods (38) we could not to accurately determine the abundance of this short-living phospholipid (Fig. 5 B and D).

In conclusion, there was a normal qualitative lipid composition of human WAT from lipin-1 defective patients.

Expression analysis of key adipogenic genes in fat biopsies from lipin-1 defective patients.

We performed gene expression analysis in the adipose tissue from lipin-1 defective patients, with emphasis on some pivotal determinants and regulators of adipogenesis, namely *SREBF1* (SREBP1), *PPARG* (PPAR γ) and *PGC1A* (PGC-1 α), which have been involved in the maintenance of the mature adipose phenotype and are potential lipin-1 transcriptional targets (Fig. 6 A-C) (48-50).

Unexpectedly, we found that fat biopsies from lipin-1 defective patients express significantly higher levels of two key transcription factors regulated by CCAAT/enhancer binding proteins, *PPARG*, *SREBF1* and of *PGC1A*, compared with normal controls (Fig. 6 A-C). SREBP1 and PPAR γ have an established role in FA biosynthesis and adipocyte differentiation (49), are subjected to transcriptional co-activation by PGC-1 α (48, 50), and their impairment has been directly associated to congenital forms of lipodystrophy (51, 52). Therefore, our observations indicate that a specific compensatory phenomenon can be activated in vivo in human adipocytes in the presence of depleted lipin-1 expression.

Induction of adipogenic differentiation in human dermal fibroblasts populations isolated from patients carrying biallelic *LPIN1* mutations.

Lipin-1 plays an established role in the regulation of mouse adipogenic differentiation (3, 7, 14, 53), and primary mouse embryonic fibroblasts derived from lipin-1-deficient mice [*Lpin1*^(fl/fl) mice] display a severely impaired adipogenic differentiation (3).

In this study, we established primary human dermal fibroblasts (HDF) populations from lipin-1 defective patients and from control individuals. It has been shown that HDF populations possess a mesenchymal potential, and can be committed to adipogenic differentiation in the presence of an appropriate differentiation medium (DM) containing a combination of insulin, glucocorticoids and pharmacological compounds that increase the intracellular cAMP (54, 55). Previous investigations showed variable degrees of mesenchymal potential in HDF populations isolated from different individuals (56, 57), and this likely depends on the variable fraction of mesenchymal stem cells (MSC) in the diverse HDF cellular preparations.

Consistently, as shown in Fig. 7, we observed that all the different HDF populations (that we isolated from patients or controls, see Table 1) expressed significant levels of genes encoding the MSC-specific surface markers [VCAM-1 (CD106), MCAM (CD146) and ITGA11 (56, 57, 58)], even if there was an ample heterogeneity in the expression levels of these genes between the various HDF populations (Fig. 7). The same primary HDF populations also expressed MME (CD10) and DPP4 (CD26), which are considered to be fibroblast-specific cell surface markers (Fig. 7) (58). Therefore, all the HDF populations we isolated could potentially exhibit a mesenchymal differentiation capacity, and be potentially committed to adipogenic differentiation.

All of the HDF populations derived from lipin-1 defective patients or normal control individuals, when exposed to adipogenic DM, progressively expressed *PPARG*, *FASN* and *PGC1A* (Fig. 8), which are key markers of adipogenic differentiation (48, 49, 50, 59). This increased expression of adipogenic markers during the progression of the differentiation was associated with a late and sporadic (i.e. in less than 10% of the confluent cells) accumulation of intracellular lipid droplets, in the late differentiation times (later than 8 days in DM, results not shown).

These results show that the impairment of lipin-1 in primary human pre-adipogenic cell populations does not affect the induction of key transcriptional events that characterize the multistep process of adipogenic

differentiation (Fig. 8). They also show that there was a significant gene expression of the *bona fide*-considered MSC-specific markers (such as *VCAM-1*, *MCAM* and *ITGA11*) in primary HDF populations, which could be a sufficient predictive indicator of the adipogenic potential (57, 58). Further experiments are required to assess whether the expression of this cluster of MSC-specific markers can also outline the mesenchymal multipotency of primary HDF populations.

DISCUSSION

We used human fat biopsies from patients carrying inactivating mutations in the *LPIN1* gene in both alleles to explore whether impairment of lipin-1 is associated with metabolic, developmental or histopathological defects that can be ascribed to lipodystrophy or adipose tissue deficiencies. Acquired or congenital lipodystrophies are a clinically and genetically heterogeneous group of metabolic disorders, characterized by either a partial or a generalized lack of adipose tissue (51, 52, 60). Lipodystrophies are typically associated with dyslipidemia, fatty liver, insulin resistance, diabetes and cardiovascular disease (21, 60, 61). Some underlying genetic defects observed in the lipodystrophies are directly related to adipocyte development such as mutations in the gene encoding for the transcription factor PPAR γ (51). Mutations in the gene associated with glycerolipid synthesis such as *AGPAT2* (1-acylglycerol-3-phosphate O-acyltransferase 2, also known as *BSCL1*) are associated with the congenital generalized lipodystrophy (CGL), or Berardinelli-Seip syndrome. This is a very severe form of generalized human lipodystrophy, characterized by the virtual absence of adipose tissue and a severe insulin resistance (21). *AGPAT2* encodes an enzyme located within the endoplasmic reticulum (ER) that converts lysophosphatate to phosphatate, the second step in de novo phospholipid biosynthesis. Mutations in the gene known as *BSCL2*, are involved in the type 2-Berardinelli-Seip congenital lipodystrophy (62). Interestingly, *BSCL2* encodes seipin, a transmembrane protein localized to the ER which can bind lipin-1 (63).

LPIN1 is a top-rank candidate gene for human congenital lipodystrophy. Lipin-1 dephosphorylates PA to DAG, a common precursor for TAG and PL synthesis (64), acting in the metabolic pathway immediately downstream of *AGPAT2*. Therefore, the gene products of *AGPAT*, *LPIN1* and *BSCL2* are closely functionally or physically associated, explaining how mutations in each of these genes can be directly correlated to lipodystrophy. The *Lpin1* gene is prevalently expressed in white and brown adipose tissue, and in skeletal and cardiac muscles, that are all tissues characterized by active TAG synthesis and/or by a high capacity β -oxidation (13, 64, 65). It has been shown that: i) adipocyte-specific *Lpin1* knockout mouse models, ii) *Lpin1*^(*fld/fld*) mice, carrying spontaneous inactivation of the *Lpin1* gene, and iii) *Lpin1*^{*1Hubr*} rats with a mutated lipin-1 protein, all unambiguously display lipodystrophy (even if each animal model is characterized by different penetrance and severity of the pathological phenotype) (1, 2, 7, 14, 24, 53). The single lipin protein orthologue in *Drosophila*

(encoded by *dLipin*) is also essential for normal fat body development, and for normal lipid accumulation and TAG storage in the lipid droplets of the adipocytes (66).

Although loss of lipin-1 in mouse models leads to manifest lipodystrophy, hepatic steatosis and insulin resistance, so far none of these pathological conditions have also been observed in human individuals deficient in lipin-1, who have normal adipose tissue distribution and fat weight (27, 28, 32). Instead, we and others showed that deleterious *LPIN1* mutations cause recurrent severe paediatric clinical episodes of rhabdomyolysis, a syndrome consisting in massive breakdown of skeletal muscle fibers, leading to myoglobinuria (27, 29, 32). The clinical features of rhabdomyolysis observed in human lipin-1-defective patients are compatible with that observed in *Lpin1*^(fla/fla) mice models subjected to specific metabolic stress, in which skeletal muscle myofibrillar necrosis was also evident, due to impairment of mitochondrial functions and autophagy (30).

Until now, a thorough and systematic analysis of human adipose tissue from patients harboring *LPIN1* inactivating mutations was not performed. We established that the WAT tissue from these patients: i) is characterized by severely reduced levels of *LPIN1* mRNA, lipin-1 protein and PAP activity, without the concomitant compensatory increased expression of *LPIN2* and *LPIN3*; ii) does not show any of the typical histopathological features associated with lipodystrophy (i.e: hypoplastic development, inflammation, increased mixoid stroma, abnormal lipid droplets, abnormal vasculature); iii) shows a moderate reduction of adipocyte size, indicative of a possible decreased capacity of fat accumulation in the lipid droplets; iv) has a normal qualitative composition of the stored lipids; v) express significantly higher levels of the key positive regulators of the adipogenesis *SREBF1*, *PPARG* and *PGCIA*.

The observation that human adipose tissue in lipin-1 deficient patients can develop fully and store neutral lipids normally, can be explained if some specific compensatory phenomena were triggered in human adipocytes. In agreement with this hypothesis, here we showed that fat biopsies from lipin-1 defective patients express significantly higher levels of *SREBP1*, *PPARG* and *PGCAI*, three pivotal determinants of the adipogenesis (64, 67). Also, mesenchymal populations derived from lipin-1-defective patients recapitulate the key transcriptional events that characterize the multistep process of adipogenic differentiation. These results agree with our previous experimental observations, showing that PPAR/PGC-1 α mediated-adipogenesis is

increased in human lipin-1-deficient myoblasts (29), and also with our description of an autaptic case of a young lipin-1 defective patient with an associated severe cardiac infiltration with adipocytes (68). This would be consistent with an increased adipogenesis induced by *SREBP1*, *PPARG* and *PGC1A* upregulation.

We established that lipin-1 accounts for the majority of PAP activity in human WAT, and that the inactivating mutations are compatible with a normal human adipose tissue differentiation and functions. In agreement with this, depletion of lipin-1 by siRNA in the human pre-adipocytic SGBS cell line leads to about 95% of depletion of PAP activity without impairing adipogenic differentiation and accumulation of neutral lipids (31). By contrast to what we observed in WAT of human patients carrying biallelic inactivating mutations in *LPIN1*, repression of lipin-1 in SGBS cells caused a significant reduction of the key adipogenic transcription factors *PPARG* and *SREBP1* (31).

The lipin paralogues lipin-1, -2 and -3 share homologous sequences, and overlapping PAP enzymatic functions (9). Lipin-2 and -3 can potentially compensate for the absence of lipin-1 (9, 25, 69). Previous studies with 3T3-L1 mouse preadipocyte cells showed that lipin-1 is progressively expressed during differentiation in culture (6), and lipin-1 depletion after the initiation of the adipogenesis results in increased expression of lipin-2 (but not of lipin-3) (26). However, in the present study we showed that the severe deficiency of lipin-1 and of PAP activity in human adipose tissue was not compensated by an increased expression of *LPIN2* (Fig. 6), and *LPIN3* expression was never detectable in human adipose tissue of patients or controls (results not shown).

Virtually no PAP activity was reported in WAT and in skeletal muscle from lipin-1 deficient [*Lpin1*^(fl^d/fl^d)] mice (9). These results probably depend on the composition of the PAP assay since adjusting the Mg²⁺ concentration and the pH in the PAP assay revealed that hearts of *Lpin1*^(fl^d/fl^d) mice still retain about 15-20% of the PAP activity of the controls (25), and this was sufficient to sustain normal rates of TAG synthesis and β -oxidation in perfused working hearts, even though there was cardiac dysfunction (25). It was concluded that PAP activity is normally present in excess in the mouse cardiac tissue, and that lipins-2 and -3 were able to compensate for the complete loss of lipin-1 in the *Lpin1*^(fl^d/fl^d) hearts (25).

In the present study we used the same PAP assay used in (25) and found that WAT biopsies from lipin-1 defective patients displayed, on average, about 13% of the PAP activity of the controls. Consistent with this, we

previously showed a severe reduction of the cellular PAP activity in primary myoblasts established from lipin-1 defective patients carrying different types of *LPIN1* mutant alleles (29), but we also observed that all of primary myoblasts analyzed still retained a significant cellular PAP activity (29). We conclude that the significant residual PAP activity in WAT of lipin-1 deficient patients (Fig. 4 C) depends on the low (but significant) expression of *LPIN2* in this tissue (Fig. 6). This is substantiated also by the weak residual band on the Western blots of WAT from patients, as shown in Fig. 4 A and B, since the antibody anti-human lipin-1 we used cross reacts with lipin-2 (see Methods). Using the same antibody anti-lipin-1, a residual weak protein band of about 100 kDa was also detected in Western blots of myoblasts established from the patients analyzed in this work (result not shown). The expression of lipin-2 in human adipose tissue of patients carrying lipin-1 inactivating mutations could be sufficient to sustain a normal TAG synthesis and adipogenesis. This would explain the difference between the mouse and human phenotype in absence of a functional lipin-1.

Lipin-1 is a multifunctional protein that can regulate lipid metabolism at several levels (5, 10, 11-13). Under physiological conditions and in response to increased fatty acid delivery, lipin-1 dependent PAP activity can play a specialized role to rapidly increase the esterification of fatty acids into TAG in the adipose tissue, whereas the lipin-1 gene regulatory effects (mediated by PGC-1 α) appear to be particularly prominent in the liver, supporting the hepatic capacity for β -oxidation (FAO) and suppressing the hepatic fatty acid synthesis (13). The evidence that we have presented suggests under homeostatic conditions that the WAT in lipin-1 defective patients shows a virtually normal metabolic lipid balance, without any evident accumulation of unesterified fatty acids (Fig. 5). Possibly, if these patients were challenged by circumstances of increased fatty acid delivery (such as fasting, diabetes, a diet rich in fat, alcohol assumption), they would show the symptoms of impaired capacity for fatty acid esterification in WAT, with a consequent accumulation of unesterified fatty acids.

Theoretically, LPP activity could compensate the severe PAP defect that is observed in patients. However it was shown in *Lpin1*^{Hubr} rat model of PAP-deficiency, that the compensatory increase of LPP was restricted to the sciatic nerve endoneurium, but was not detectable in WAT (24). Also in the *Lpin1*^(Ndf/d) mice, no significant difference in LPP activity was found in WAT (23). Furthermore, the location of the catalytic site of

the LPPs on the outer surface of the plasma membrane, or on the luminal surface of internal membranes, make it unlikely that the PA formed during lipid synthesis in the ER could be available directly to the LPPs (70).

Lipin-1 catalyzes a crucial step in triacylglycerol (TAG) biosynthesis, which agrees with reduced neutral lipid storage and accumulation of PA that has been observed in lipin-1 deficient mouse (2, 5, 7, 14, 16, 22-24). Analysis of the lipids in muscle of *Lpin1*^(fl^d/fl^d) mice showed accumulation of high levels of various phospholipids (PL) and unesterified FA, that could contribute to altered metabolism in lipin-1-deficient muscles (30). Our analysis of WAT biopsies revealed that patients carrying inactivating mutations of the *LPINI* gene are not characterized by altered relative proportions between TAG and PL, or by altered relative proportion of the long chain FA in the TAG, or by abnormal accumulation of unesterified FA or phospholipids (Fig. 5).

We found a significant, but moderate, reduction in adipocyte size in lipin-1 deficient patients compared with normal controls, which could be symptomatic of a reduced capacity for neutral lipid storage in the lipid droplets in these patients. However, we cannot completely exclude the possibility that the reduced adipocyte size might depend on other confounding factors (age, genetic background, environmental factors, etc.) or adaptations of the energy balance linked to muscle alteration in patients. Accumulation of neutral lipids is determined by a balance among lipid biosynthesis, lipid hydrolysis and β -oxidation. Therefore, further analysis is required to explore the hypothesis that other non-lipin-dependent compensatory pathways, like the monoacylglycerol O-acyltransferase (MOGAT) pathway (71), or the downregulation of the lipid hydrolysis and FAO, may contribute to compensate the deficiency of lipin-1 in human patients.

In summary, adipose tissue from patients with biallelic *LPINI* inactivating mutations displays a dramatic reduction in lipin-1 levels and PAP activity. Nevertheless, the adipose tissue appeared to develop normally, without manifest signs of lipodystrophy and with a normal qualitative composition of the storage lipids. The overexpression of key adipogenic determinants such as *SREBP1*, *PPARG* and *PGC1A* and the residual PAP activity suggest that specific compensatory phenomena should be activated in human adipocytes in the presence of lipin-1 depletion. Additional work is required to decipher the exact nature of this compensation program. This paper highlights the evidence that human beings and mice can exhibit very important patho-physiological differences, despite the very high conservation of the genomes, and despite the high similarity in the

transcriptional landscapes, gene regulation machinery and metabolic networks. In particular, the penetrance of deleterious mutations in metabolic genes can depend strongly on the activation of compensatory phenomena, such as metabolic and genetic regulations, expression of paralogues genes, etc., in association with environmental factors.

ACKNOWLEDGMENTS/GRANT SUPPORT

We thank Dr Giulia Bolasco and Dr Federico Ceriani for their critical reading of this manuscript and their helpful comments. We thank Dr Asmaa Mamoune, Luc Nonnemacher and Asma Smahi for technical assistance and support. This work was supported by Agence Nationale de la Recherche (ANR-13-BSV1-0020-01), the Association Française contre les Myopathies (grant numbers 13988, 15947), the Fondation Bettencourt (2012), the Fondation de l'Avenir (grant number 09071), the Fondation Lejeune (grant 2014), the Fondation Maladies Rares, Patient associations (Nos Anges, AMMI, Hyperinsulinisme, and Noa Luû) and the Canadian Breast Cancer Foundation.

REFERENCES

1. Langner, C. A., E. H. Birkenmeier, O. Ben-Zeev, M. C. Schotz, H. O. Sweet, M. T. Davisson, and J. I. Gordon. 1989. The fatty liver dystrophy (fld) mutation. A new mutant mouse with a developmental abnormality in triglyceride metabolism and associated tissue-specific defects in lipoprotein lipase and hepatic lipase activities. *J. Biol. Chem.* **264**: 7994-8003.
2. Reue, K. 2007. The role of lipin 1 in adipogenesis and lipid metabolism. *Novartis Found. Symp.* **286**: 58-68; discussion 68-71, 162-163, 196-203.
3. Phan, J., M. Peterfy, and K. Reue. 2004. Lipin expression preceding peroxisome proliferator-activated receptor-gamma is critical for adipogenesis in vivo and in vitro. *J. Biol. Chem.* **279**: 29558-29564.
4. Phan, J., M. Peterfy, and K. Reue. 2005. Biphasic expression of lipin suggests dual roles in adipocyte development. *Drug news perspect.* **18**: 5-11.
5. Mitra, M. S., Z. Chen, H. Ren, T. E. Harris, K. T. Chambers, A. M. Hall, K. Nadra, S. Klein, R. Chrast, X. Su, A. J. Morris, and B. N. Finck. 2013. Mice with an adipocyte-specific lipin 1 separation-of-function allele reveal unexpected roles for phosphatidic acid in metabolic regulation. *Proc. Natl. Acad. Sci. U.S.A.* **110**: 642-647.
6. Peterfy, M., J. Phan, and K. Reue. 2005. Alternatively spliced lipin isoforms exhibit distinct expression pattern, subcellular localization, and role in adipogenesis. *J. Biol. Chem.* **280**: 32883-32889.
7. Peterfy, M., J. Phan, P. Xu, and K. Reue. 2001. Lipodystrophy in the fld mouse results from mutation of a new gene encoding a nuclear protein, lipin. *Nat. Genet.* **27**: 121-124.
8. Han, G. S., W. I. Wu, and G. M. Carman. 2006. The *Saccharomyces cerevisiae* Lipin homolog is a Mg²⁺-dependent phosphatidate phosphatase enzyme. *J. Biol. Chem.* **281**: 9210-9218.
9. Donkor, J., M. Sariahmetoglu, J. Dewald, D. N. Brindley, and K. Reue. 2007. Three mammalian lipins act as phosphatidate phosphatases with distinct tissue expression patterns. *J. Biol. Chem.* **282**: 3450-3457.
10. Pascual, F., and G. M. Carman. 2013. Phosphatidate phosphatase, a key regulator of lipid homeostasis. *Biochim. Biophys. Acta* **183**: 514-522.
11. Sugden, M. C., P. W. Caton, and M. J. Holness. 2010. PPAR control: it's SIRTainly as easy as PGC. *J. Endocrinol.* **204**: 93-104.

12. Peterson, T. R., S. S. Sengupta, T. E. Harris, A. E. Carmack, S. A. Kang, E. Balderas, D. A. Guertin, K. L. Madden, A. E. Carpenter, B. N. Finck, and D. M. Sabatini. 2011. mTOR complex 1 regulates lipin 1 localization to control the SREBP pathway. *Cell* **146**: 408-420.
13. Finck, B. N., M. C. Gropler, Z. Chen, T. C. Leone, M. A. Croce, T. E. Harris, J. C. Lawrence, Jr., and D. P. Kelly. 2006. Lipin 1 is an inducible amplifier of the hepatic PGC-1alpha/PPARalpha regulatory pathway. *Cell Metab.* **4**: 199-210.
14. Nadra, K., J. J. Medard, J. D. Mul, G. S. Han, S. Gres, M. Pende, D. Metzger, P. Chambon, E. Cuppen, J. S. Saulnier-Blache, G. M. Carman, B. Desvergne, and R. Chrast. 2012. Cell autonomous lipin 1 function is essential for development and maintenance of white and brown adipose tissue. *Mol. Cell. Biol.* **32**: 4794-4810.
15. Kim, H. B., A. Kumar, L. Wang, G. H. Liu, S. R. Keller, J. C. Lawrence, Jr., B. N. Finck, and T. E. Harris. 2010. Lipin 1 represses NFATc4 transcriptional activity in adipocytes to inhibit secretion of inflammatory factors. *Mol. Cell. Biol.* **30**: 3126-3139.
16. Mitra, M. S., Z. Chen, H. Ren, T. E. Harris, K. T. Chambers, A. M. Hall, K. Nadra, S. Klein, R. Chrast, X. Su, A. J. Morris, and B. N. Finck. 2013. Mice with an adipocyte-specific lipin 1 separation-of-function allele reveal unexpected roles for phosphatidic acid in metabolic regulation. *Proc. Natl. Acad. Sci. U.S.A.* **110**: 642-647.
17. Rehnmark, S., C. S. Giometti, B. G. Slavin, M. H. Doolittle, and K. Reue. 1998. The fatty liver dystrophy mutant mouse: microvesicular steatosis associated with altered expression levels of peroxisome proliferator-regulated proteins. *J. Lipid Res.* **39**: 2209-2217.
18. Reue, K., and P. Zhang. 2008. The lipin protein family: dual roles in lipid biosynthesis and gene expression. *FEBS Lett.* **582**: 90-96.
19. Kanda, H., S. Tateya, Y. Tamori, K. Kotani, K. Hiasa, R. Kitazawa, S. Kitazawa, H. Miyachi, S. Maeda, K. Egashira, and M. Kasuga. 2006. MCP-1 contributes to macrophage infiltration into adipose tissue, insulin resistance, and hepatic steatosis in obesity. *J. Clin. Invest.* **116**: 1494-1505.

20. Meana, C., L. Pena, G. Lorden, E. Esquinas, C. Guijas, M. Valdearcos, J. Balsinde, and M. A. Balboa. 2014. Lipin-1 Integrates Lipid Synthesis with Proinflammatory Responses during TLR Activation in Macrophages. *J. Immunol.* **193**: 4614-4622.
21. Agarwal, A. K., E. Arioglu, S. De Almeida, N. Akkoc, S. I. Taylor, A. M. Bowcock, R. I. Barnes, and A. Garg. 2002. AGPAT2 is mutated in congenital generalized lipodystrophy linked to chromosome 9q34. *Nat. Genet.* **31**: 21-23.
22. Takeuchi, K., and K. Reue. 2009. Biochemistry, physiology, and genetics of GPAT, AGPAT, and lipin enzymes in triglyceride synthesis. *Am. J. Physiol. Endocrinol. Metab.* **296**: E1195-1209.
23. Nadra, K., A. S. de Preux Charles, J. J. Medard, W. T. Hendriks, G. S. Han, S. Gres, G. M. Carman, J. S. Saulnier-Blache, M. H. Verheijen, and R. Chrast. 2008. Phosphatidic acid mediates demyelination in Lpin1 mutant mice. *Genes Dev.* **22**: 1647-1661.
24. Mul, J. D., K. Nadra, N. B. Jagalur, I. J. Nijman, P. W. Toonen, J. J. Medard, S. Gres, A. de Bruin, G. S. Han, J. F. Brouwers, G. M. Carman, J. S. Saulnier-Blache, D. Meijer, R. Chrast, and E. Cuppen. 2011. A hypomorphic mutation in Lpin1 induces progressively improving neuropathy and lipodystrophy in the rat. *J. Biol. Chem.* **286**: 26781-26793.
25. Kok, B. P., P. C. Kienesberger, J. R. Dyck, and D. N. Brindley. 2012. Relationship of glucose and oleate metabolism to cardiac function in lipin-1 deficient (fld) mice. *J. Lipid Res.* **53**: 105-118.
26. Sembongi, H., M. Miranda, G. S. Han, S. Fakas, N. Grimsey, J. Vendrell, G. M. Carman, and S. Siniosoglou. 2013. Distinct roles of the phosphatidate phosphatases lipin 1 and 2 during adipogenesis and lipid droplet biogenesis in 3T3-L1 cells. *J. Biol. Chem.* **288**: 34502-34513.
27. Zeharia, A., A. Shaag, R. H. Houtkooper, T. Hindi, P. de Lonlay, G. Erez, L. Hubert, A. Saada, Y. de Keyzer, G. Eshel, F. M. Vaz, O. Pines, and O. Elpeleg. 2008. Mutations in LPIN1 cause recurrent acute myoglobinuria in childhood. *Am. J. Hum. Genet.* **83**: 489-494.
28. Michot, C., L. Hubert, M. Brivet, L. De Meirleir, V. Valayannopoulos, W. Muller-Felber, R. Venkateswaran, H. Ogier, I. Desguerre, C. Altuzarra, E. Thompson, M. Smitka, A. Huebner, M. Husson, R. Horvath, P.

- Chinnery, F. M. Vaz, A. Munnich, O. Elpeleg, A. Delahodde, Y. de Keyzer, and P. de Lonlay. 2010. LPIN1 gene mutations: a major cause of severe rhabdomyolysis in early childhood. *Hum. Mutat.* **31**: E1564-1573.
29. Michot, C., A. Mamoune, J. Vamecq, M. T. Viou, L. S. Hsieh, E. Testet, J. Laine, L. Hubert, A. F. Dessein, M. Fontaine, C. Ottolenghi, L. Fouillen, K. Nadra, E. Blanc, J. Bastin, S. Candon, M. Pende, A. Munnich, A. Smahi, F. Djouadi, G. M. Carman, N. Romero, Y. de Keyzer, and P. de Lonlay. 2013. Combination of lipid metabolism alterations and their sensitivity to inflammatory cytokines in human lipin-1-deficient myoblasts. *Biochim. Biophys. Acta* **1832**: 2103-2114.
30. Zhang, P., M. A. Verity, and K. Reue. 2014. Lipin-1 Regulates Autophagy Clearance and Intersects with Statin Drug Effects in Skeletal Muscle. *Cell Metab.* **20**: 267-279.
31. Temprano, A., H. Sembongi, G. S. Han, D. Sebastian, J. Capellades, C. Moreno, J. Guardiola, M. Wabitsch, C. Richart, O. Yanes, A. Zorzano, G. M. Carman, S. Siniossoglou, and M. Miranda. 2016. Redundant roles of the phosphatidate phosphatase family in triacylglycerol synthesis in human adipocytes. *Diabetologia* **59**: 1985-1994.
32. Michot, C., L. Hubert, N. B. Romero, A. Gouda, A. Mamoune, S. Mathew, E. Kirk, L. Viollet, S. Rahman, S. Bekri, H. Peters, J. McGill, E. Glamuzina, M. Farrar, M. von der Hagen, I. E. Alexander, B. Kirmse, M. Barth, P. Laforet, P. Benlian, A. Munnich, M. Jeanpierre, O. Elpeleg, O. Pines, A. Delahodde, Y. de Keyzer, and P. de Lonlay. 2012. Study of LPIN1, LPIN2 and LPIN3 in rhabdomyolysis and exercise-induced myalgia. *J. Inherit. Metab. Dis.* **35**: 1119-1128.
33. Briand, N., S. Le Lay, W. C. Sessa, P. Ferre, and I. Dugail. 2011. Distinct roles of endothelial and adipocyte caveolin-1 in macrophage infiltration and adipose tissue metabolic activity. *Diabetes* **60**: 448-453.
34. Pelosi, M., Alfò, M., Martella, F., Pappalardo, E., and A. Musarò 2015. Finite mixture clustering of human tissues with different levels of IGF-1 splice variants mRNA transcripts. *BMC Bioinformatics.* **16**:289.
35. Galanos, D.S., and V.M Kapoulas. 1965. Preparation and analysis of lipid extracts from milk and other tissues. *Biochim. Biophys. Acta* **98**: 278-292.

36. Juguelin, H., A. Heape, F. Boiron, and C. Cassagne. 1986. A quantitative developmental study of neutral lipids during myelinogenesis in the peripheral nervous system of normal and trembler mice. *Brain Res.* **390**: 249-252.
37. Vitiello, F., and J. P. Zanetta. 1978. Thin-layer chromatography of phospholipids. *J. Chromatogr.* **166**: 637-640.
38. Handloser, D., Widmer, V., and E. Reich. 2008 Separation of Phospholipids by HPTLC – An Investigation of Important Parameters. *J. of Liq. Chromatogr. & Relat. Technol.* **31**, iss.13.
39. Testet, E., J. Laroche-Traineau, A. Noubhani, D. Coulon, O. Bunoust, N. Camougrand, S. Manon, R. Lessire, and J. J. Bessoule. 2005. Ypr140wp, 'the yeast tafazzin', displays a mitochondrial lysophosphatidylcholine (lyso-PC) acyltransferase activity related to triacylglycerol and mitochondrial lipid synthesis. *Biochem. J.* **387**: 617-626.
40. Mamoune, A., Bahuau, M., Hamel, Y., Serre, V., Pelosi, M., Habarou, F., Nguyen Morel, M. A., Boisson, B., Vergnaud, S., Viou, M.T., Nonnenmacher, L., Piraud, M., Nusbaum, P., Vamecq, J., Romero, N., Ottolenghi, C., Casanova, J. L., and P. de Lonlay. 2014. A thermolabile aldolase A mutant causes fever-induced recurrent rhabdomyolysis without hemolytic anemia. *PLoS Genet.* **10**(11):e1004711.
41. Pelosi, M., De Rossi, M., Barberi, L., and A. Musarò. 2014. IL-6 impairs myogenic differentiation by downmodulation of p90RSK/eEF2 and mTOR/p70S6K axes, without affecting AKT activity. *Biomed. Res. Int.* 2014:206026.
42. Winkelmann, R. K., and E. Frigas. 1986. Eosinophilic panniculitis: a clinicopathologic study. *J. of cutaneous pathol.* **13**: 1-12.
43. Greenberg, A. S., J. J. Egan, S. A. Wek, N. B. Garty, E. J. Blanchette-Mackie, and C. Londos. 1991. Perilipin, a major hormonally regulated adipocyte-specific phosphoprotein associated with the periphery of lipid storage droplets. *J. Biol. Chem.* **266**: 11341-11346.
44. Hentze, M. W., and A. E. Kulozik. 1999. A perfect message: RNA surveillance and nonsense-mediated decay. *Cell* **96**: 307-310.

45. Dwyer, J. R., J. Donkor, P. Zhang, L. S. Csaki, L. Vergnes, J. M. Lee, J. Dewald, D. N. Brindley, E. Atti, S. Tetradis, Y. Yoshinaga, P. J. De Jong, L. G. Fong, S. G. Young, and K. Reue. 2012. Mouse lipin-1 and lipin-2 cooperate to maintain glycerolipid homeostasis in liver and aging cerebellum. *Proc. Natl. Acad. Sci. U.S.A.* **109**: E2486-2495.
46. Wu, C., C. Orozco, J. Boyer, M. Leglise, J. Goodale, S. Batalov, C. L. Hodge, J. Haase, J. Janes, J. W. Huss, 3rd, and A. I. Su. 2009. BioGPS: an extensible and customizable portal for querying and organizing gene annotation resources. *Genome Biol.* **10**: R130.
47. Morita, S. Y., Ueda, K., and S. Kitagawa. 2009. Enzymatic measurement of phosphatidic acid in cultured cells. *J. Lipid Res.* **50**:1945-1952.
48. Rosen, E. D., C. H. Hsu, X. Wang, S. Sakai, M. W. Freeman, F. J. Gonzalez, and B. M. Spiegelman. 2002. C/EBPalpha induces adipogenesis through PPARgamma: a unified pathway. *Genes Dev.* **16**: 22-26.
49. Kim, J. B., P. Sarraf, M. Wright, K. M. Yao, E. Mueller, G. Solanes, B. B. Lowell, and B. M. Spiegelman. 1998. Nutritional and insulin regulation of fatty acid synthetase and leptin gene expression through ADD1/SREBP1. *J. Clin. Invest.* **101**: 1-9.
50. Summermatter, S., O. Baum, G. Santos, H. Hoppeler, and C. Handschin. 2010. Peroxisome proliferator-activated receptor {gamma} coactivator 1 {alpha} (PGC-1 {alpha}) promotes skeletal muscle lipid refueling in vivo by activating de novo lipogenesis and the pentose phosphate pathway. *J. Biol. Chem.* **285**: 32793-32800.
51. Hegele, R. A., H. Cao, C. Frankowski, S. T. Mathews, and T. Leff. 2002. PPARG F388L, a transactivation-deficient mutant, in familial partial lipodystrophy. *Diabetes* **51**: 3586-3590.
52. Agarwal, A. K., and A. Garg. 2002. A novel heterozygous mutation in peroxisome proliferator-activated receptor-gamma gene in a patient with familial partial lipodystrophy. *J. Clin. Endocrinol. Metab.* **87**: 408-411.
53. Reue, K., P. Xu, X. P. Wang, and B. G. Slavin. 2000. Adipose tissue deficiency, glucose intolerance, and increased atherosclerosis result from mutation in the mouse fatty liver dystrophy (fld) gene. *J. Lipid Res.* **41**: 1067-1076.
54. Russell, T. R., and R. Ho. 1976. Conversion of 3T3 fibroblasts into adipose cells: triggering of differentiation by prostaglandin F2alpha and 1-methyl-3-isobutyl xanthine. *Proc. Natl. Acad. Sci. U.S.A.* **73**: 4516-4520.

55. Haniffa, M. A., X. N. Wang, U. Holtick, M. Rae, J. D. Isaacs, A. M. Dickinson, C. M. Hilkens, and M. P. Collin. 2007. Adult human fibroblasts are potent immunoregulatory cells and functionally equivalent to mesenchymal stem cells. *J. Immunol.* **179**: 1595-1604.
56. Brendel, C., L. Kuklick, O. Hartmann, T. D. Kim, U. Boudriot, D. Schwell, and A. Neubauer. 2005. Distinct gene expression profile of human mesenchymal stem cells in comparison to skin fibroblasts employing cDNA microarray analysis of 9600 genes. *Gene Expr.* **12**: 245-257.
57. Halfon, S., N. Abramov, B. Grinblat, and I. Ginis. 2011. Markers distinguishing mesenchymal stem cells from fibroblasts are downregulated with passaging. *Stem Cells Dev.* **20**: 53-66.
58. Cappellesso-Fleury, S., B. Puissant-Lubrano, P. A. Apoil, M. Titeux, P. Winterton, L. Casteilla, P. Bourin, and A. Blancher. 2010. Human fibroblasts share immunosuppressive properties with bone marrow mesenchymal stem cells. *J. Clin. Immunol.* **30**: 607-619.
59. Kim, J. B., and B. M. Spiegelman. 1996. ADD1/SREBP1 promotes adipocyte differentiation and gene expression linked to fatty acid metabolism. *Genes Dev.* **10**: 1096-1107.
60. Agarwal, A. K., V. Simha, E. A. Oral, S. A. Moran, P. Gorden, S. O'Rahilly, Z. Zaidi, F. Gurakan, S. A. Arslanian, A. Klar, A. Ricker, N. H. White, L. Bindl, K. Herbst, K. Kennel, S. B. Patel, L. Al-Gazali, and A. Garg. 2003. Phenotypic and genetic heterogeneity in congenital generalized lipodystrophy. *J. Clin. Endocrinol. Metab.* **88**: 4840-4847.
61. Yao-Borengasser, A., N. Rasouli, V. Varma, L. M. Miles, B. Phanavanh, T. N. Starks, J. Phan, H. J. Spencer, 3rd, R. E. McGehee, Jr., K. Reue, and P. A. Kern. 2006. Lipin expression is attenuated in adipose tissue of insulin-resistant human subjects and increases with peroxisome proliferator-activated receptor gamma activation. *Diabetes* **55**: 2811-2818.
62. Magre, J., M. Delepine, E. Khallouf, T. Gedde-Dahl, Jr., L. Van Maldergem, E. Sobel, J. Papp, M. Meier, A. Megarbane, A. Bachy, A. Verloes, F. H. d'Abronzio, E. Seemanova, R. Assan, N. Baudic, C. Bourut, P. Czernichow, F. Huet, F. Grigorescu, M. de Kerdanet, D. Lacombe, P. Labrune, M. Lanza, H. Loret, F. Matsuda, J. Navarro, A. Nivelon-Chevalier, M. Polak, J. J. Robert, P. Tric, N. Tubiana-Rufi, C. Vigouroux, J. Weissenbach, S. Savasta, J. A. Maassen, O. Trygstad, P. Bogalho, P. Freitas, J. L. Medina, F. Bonnicci, B. I.

- Joffe, G. Loyson, V. R. Panz, F. J. Raal, S. O'Rahilly, T. Stephenson, C. R. Kahn, M. Lathrop, J. Capeau, and B. W. Group. 2001. Identification of the gene altered in Berardinelli-Seip congenital lipodystrophy on chromosome 11q13. *Nat. Genet.* **28**: 365-370.
63. Sim, M. F., R. J. Dennis, E. M. Aubry, N. Ramanathan, H. Sembongi, V. Saudek, D. Ito, S. O'Rahilly, S. Siniossoglou, and J. J. Rochford. 2012. The human lipodystrophy protein seipin is an ER membrane adaptor for the adipogenic PA phosphatase lipin 1. *Mol. Metab.* **2**: 38-46.
64. Donkor, J., L. M. Sparks, H. Xie, S. R. Smith, and K. Reue. 2008. Adipose tissue lipin-1 expression is correlated with peroxisome proliferator-activated receptor alpha gene expression and insulin sensitivity in healthy young men. *J. Clin. Endocrinol. Metab.* **93**: 233-239.
65. Mitra, M. S., J. D. Schilling, X. Wang, P. Y. Jay, J. M. Huss, X. Su, and B. N. Finck. 2011. Cardiac lipin 1 expression is regulated by the peroxisome proliferator activated receptor gamma coactivator 1alpha/estrogen related receptor axis. *J. Mol. Cell. Cardiol.* **51**: 120-128.
66. Ugrankar, R., Y. Liu, J. Provaznik, S. Schmitt, and M. Lehmann. 2011. Lipin is a central regulator of adipose tissue development and function in *Drosophila melanogaster*. *Mol. Cell. Biol.* **31**: 1646-1656.
67. Zhang, P., K. Takeuchi, L. S. Csaki, and K. Reue. 2012. Lipin-1 phosphatidic phosphatase activity modulates phosphatidate levels to promote peroxisome proliferator-activated receptor gamma (PPARgamma) gene expression during adipogenesis. *J. Biol. Chem.* **287**: 3485-3494.
68. Bergounioux, J., A. Brassier, C. Rambaud, O. Bustarret, C. Michot, L. Hubert, J. B. Arnoux, A. Laquerriere, S. Bekri, S. Galene-Gomez, D. Bonnet, P. Hubert, and P. de Lonlay. 2012. Fatal rhabdomyolysis in 2 children with LPIN1 mutations. *J. Pediatr.* **160**: 1052-1054.
69. Zhou, J., and T. L. Young. 2005. Evaluation of Lipin 2 as a candidate gene for autosomal dominant 1 high-grade myopia. *Gene* **352**: 10-19.
70. Kok, B. P. C., G. Venkatraman, D. Capatos, and D. N. Brindley. 2012. Unlike two peas in a pod: lipid phosphate phosphatases and phosphatidate phosphatases. *Chem. Rev.* **112**: 5121-5146.
71. Shi, Y., and D. Cheng. 2009. Beyond triglyceride synthesis: the dynamic functional roles of MGAT and DGAT enzymes in energy metabolism. *Am. J. Physiol. Endocrinol. Metab.* **297**: E10-18.

TABLES and TABLES LEGENDS

Table 1

| Individual | Specimens used in experiment: | age | sex | <i>LPIN1</i> mutations Nucleotides | <i>LPIN1</i> mutations Amino Acids |
|---------------------|-------------------------------|------|-----|--|--|
| control 1 | s.a.t.b. | 12 | F | WT | WT |
| control 2 | s.a.t.b. | 15 | F | WT | WT |
| control 3 | s.a.t.b. | 18 | M | WT | WT |
| control 4 | s.a.t.b. | 16 | M | WT | WT |
| control 5 | s.a.t.b. | 4 | M | WT | WT |
| control 6 | s.a.t.b. | 15 | M | WT | WT |
| control 7 | s.a.t.b. | 15 | M | WT | WT |
| control 8 | skin fibroblasts population | 5 | F | WT | WT |
| control 9 | skin fibroblasts population | 2.5 | M | WT | WT |
| control 10 | skin fibroblasts population | 8.5 | M | WT | WT |
| lipin-1 deficient 1 | s.a.t.b. | 5 | M | c.1162C>T c.1162C>T | p.Arg388X p.Arg388X |
| lipin-1 deficient 2 | s.a.t.b. | 5 | M | c.1441+2T>C c.2295-866_2410-30del | p.Asn417LysfsX22 p.Glu766_Ser838del |
| lipin-1 deficient 3 | s.a.t.b. | 11 | M | c.1441+2T>C c.2295-866_2410-30del | p.Asn417LysfsX22 p.Glu766_Ser838del |
| lipin-1 deficient 4 | s.a.t.b. | 47 | M | c.1162C>T c.1162C>T | p.Arg388X p.Arg388X |
| lipin-1 deficient 5 | skin fibroblasts population | 4 | F | c.2295-863_2410-27del c.2295-863_2410-27del | p.Glu766_Ser838del p.Glu766_Ser838del |
| lipin-1 deficient 6 | skin fibroblasts population | 11.5 | F | c.1441+2T>C c.2295-863_2410-27del | p.Asn417LysfsX22 p.Glu766_Ser838del |
| Lipin-1 deficient 7 | skin fibroblasts population | 4 | F | c.2295-863_2410-27del c.921delT | p.Glu766_Ser838del p.Gln308ArgfsX36 |

Table 1. Characterization of the patients and healthy controls individuals used in the study.

Legend: s.a.t.b.: subcutaneous adipose tissue biopsy.

Table 2

A) Adipocytes diameter (μm): exploratory statistics.

| Group | Min. | 1 st Qu. | Median | Mean | 3 rd Qu. | Max. |
|----------------|-------|---------------------|--------|-------|---------------------|-------|
| Controls (n=5) | 13.94 | 51.74 | 70.14 | 72.18 | 91.92 | 153.9 |
| Patients (n=4) | 10.57 | 43.93 | 58.67 | 61.25 | 77.81 | 142.2 |

B) Two-sample Kolmogorov-Smirnov test.

| | D | p-value |
|----------------------------------|-------|-----------------|
| Patients (n=4) vs Controls (n=5) | 0.174 | 4.59e-05 (***) |
| Patient 1 vs Controls (n=5) | 0.204 | 0.012 (*) |
| Patient 2 vs Controls (n=5) | 0.147 | 0.143 |
| Patient 3 vs Controls (n=5) | 0.157 | 0.092 (*) |
| Patient 4 vs Controls (n=5) | 0.417 | 1.102e-13 (***) |

Table 2. Histomorphometric analysis of the adipocytes diameters. A: Exploratory statistics for the experimentally observed adipocytes diameters. The diameters (expressed in μm) of about 100 adipocytes was measured in each histological section derived from 5 normal controls and 4 lipin-1 defective patients, and the exploratory statistics were calculated for the entire group of 5 controls and for the entire group of 4 patients. Minimum, maximum, 1st quartile, median, 3rd quartile and mean are shown for each group. **B:** The empirical cumulative distribution functions (ECDF) of the adipocytes diameters were calculated for the grouped patients (n=4) and the grouped controls (n=5), or, to minimize the possible confounding effect of age on the adipocyte size, for each patient and for the grouped controls, as shown in Fig. 3. The two-sample Kolmogorov-Smirnov (K-S) non-parametric test was applied to statistically test the null hypothesis that the values observed for the grouped patients or for each patient were drawn from the same CDF of the grouped controls. Patient 1, age 5; Patient 2, age 5; Patient 3, age 11; patient 4, age 47. Control 1, age 12; Control 2, age 15; Control 3, age 18; Control 6, age 15; Control 7, age 15 (Controls: n=5, mean age: 15; s.d. = 1.9). Significant differences are indicated by *, $P < 0.1$; ***, $P < 0.001$.

Table 3

| LCFA _{TAG} C:D | 16:0 (%) | 16:1 (%) | 18:0 (%) | 18:1 (%) | 18:2 (%) |
|-------------------------|--------------|-------------|-------------|--------------|--------------|
| <i>LPIN1</i> def. 1 | 22.82 | 3.82 | 6.37 | 50.03 | 16.96 |
| <i>LPIN1</i> def. 3 | 25.30 | 4.91 | 7.15 | 49.19 | 13.45 |
| <i>LPIN1</i> def. 4 | 28.20 | 3.10 | 5.90 | 47.10 | 15.50 |
| mean patients ± sd | 25.40 ± 2.62 | 4.00 ± 0.84 | 6.46 ± 0.65 | 48.82 ± 1.44 | 15.33 ± 1.76 |
| Control 3 | 33.30 | 4.70 | 4.90 | 46.20 | 10.60 |
| Control 5 | 26.36 | 4.29 | 8.12 | 51.69 | 9.54 |
| Control 6 | 25.71 | 4.92 | 8.41 | 51.53 | 9.43 |
| mean controls ± sd | 29.05 ± 4,28 | 4.86 ± 0.44 | 7.01 ± 1.78 | 48.74 ± 4.06 | 10.34 ± 1.20 |

Table 3. Long-chain fatty acids composition of triacylglycerols (LCFA_{TAG}) derived from lipin-1 defective patients and normal controls. Total lipid extracts were fractionated using a two-phase extraction method (35). TAG were separated by TLC as shown in Fig. 3 and LCFA_{TAG} analysed by gas chromatography. Data are presented for the different C:D (i.e. for the different lipid number, where *C* is the number of carbon atoms in the fatty acid and *D* is the number of double bonds in the fatty acid) as percent (%) of the total of LCFA_{TAG}. Mean values ± SD for the LCFA_{TAG} (%) of patients and controls are shown for each C:D.

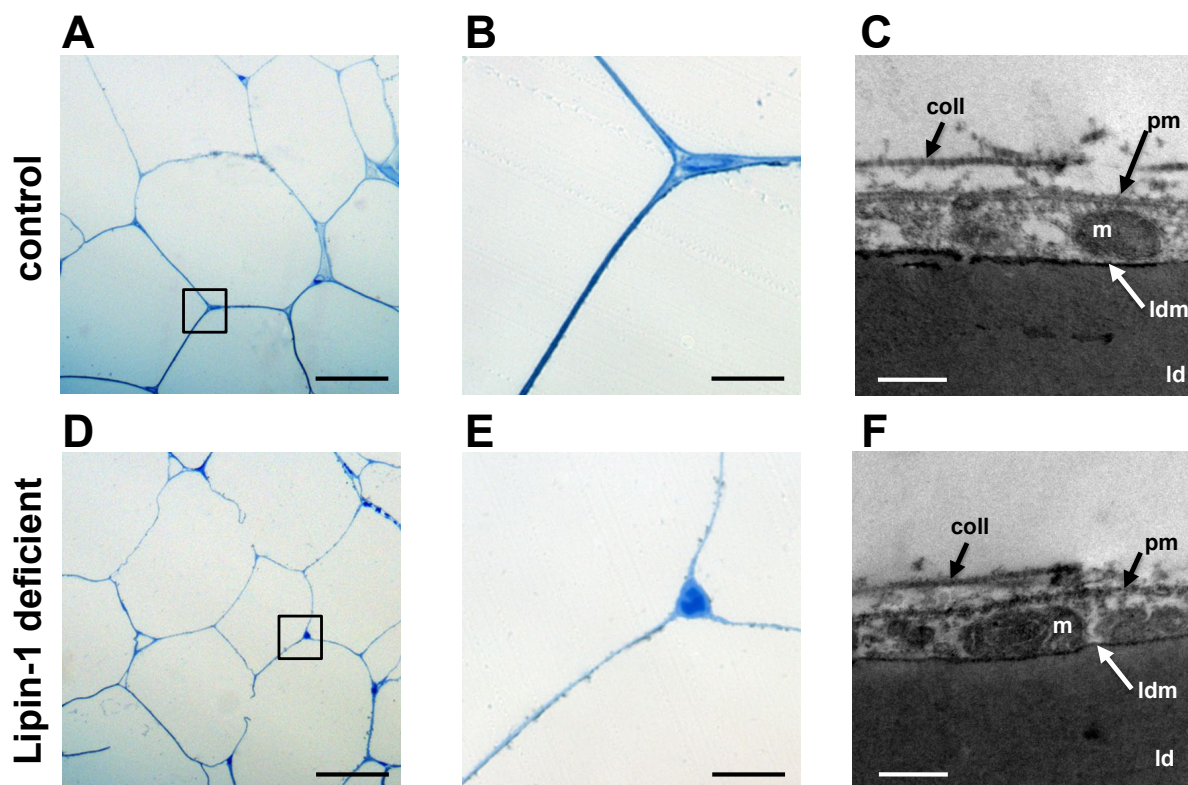


Figure 1. Histomorphometrical and ultrastructural analyses of the adipose tissue in patients carrying biallelic *LPIN1* inactivating mutations. **A, B, D** and **E**: microscopic images at low (**A, D**) and high (**B** and **E**) magnification of semi-thin sections stained with azur B-methylene blue, representative of subcutaneous adipose tissue biopsies derived from normal control individuals (**A, B**) and from lipin-1 defective patients (**D, E**), from biopsies fixed in glutaraldehyde and treated as indicated in the Methods section. No signs of lipodistrophy or perturbation of the adipose tissue morphology and organization were observed in histological sections from lipin-1 defective patients (**D, E**) compared with controls (**A, B**). Scale bars in **A** and **D**: 25 μm ; scale bars in **B** and **E**: 2.5 μm . **C** and **F**: transmission electronic microscopy (TEM) microphotographs. No signs of alteration in the adipocytes ultrastructure were observed in lipin-1 defective patients. Scale bars in **C** and **F**: 200 nm. Legend: m, mitochondria; coll, extracellular fibrillar collagen; ld, lipid droplet; pm, plasmamembrane; ldm, membrane of

the lipid droplet. The experiment shown was repeated three times using biopsies derived from three independent lipin-1 defective patients and from three independent control individuals, and gave similar results.

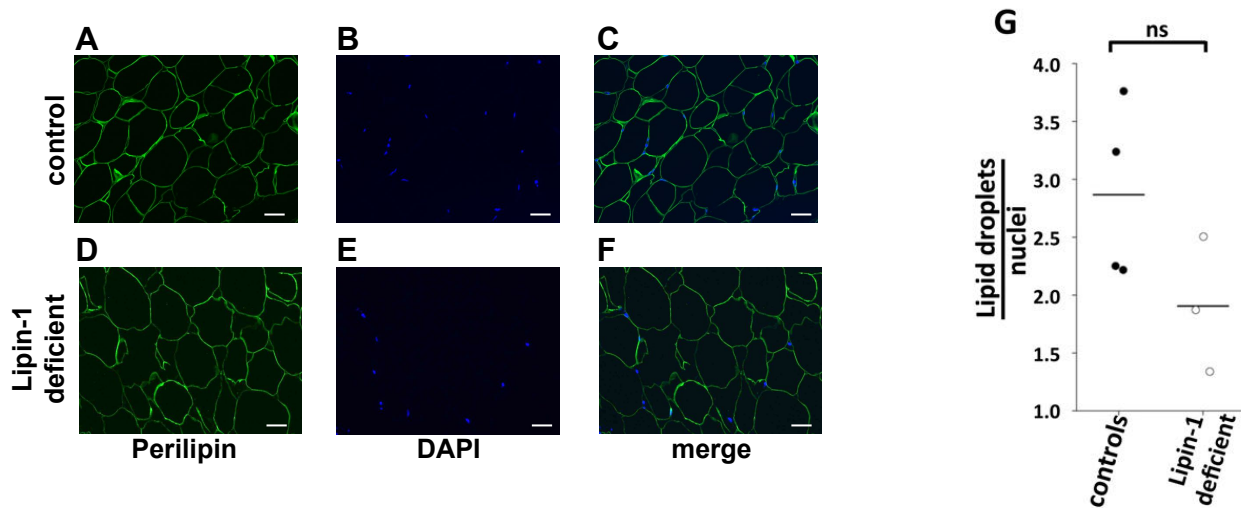


Figure 2. Histomorphometrical analysis of the adipose tissue in patients carrying biallelic *LPIN1* inactivating mutations. Histological sections from subcutaneous adipose tissue biopsies derived from lipin-1 defective patients and from controls were immunostained with an anti-perilipin antibody; the nuclei were counterstained with DAPI. The sections were subjected to immunofluorescence microscopy. Representative immunofluorescent image for a control individual (A-C) and for a lipin-1 defective patient (D-F) are shown. Perilipin cellular distribution and relative abundance did not show any significant difference in the adipose tissue from lipin-1-deficient individuals, when compared to normal controls. Anti-perilipin antibody, green; DAPI staining of the nuclei, blue; scale bars = 25 μ m. The experiment was repeated using biopsies from three independent lipin-1 defective patients and four control individuals, and gave similar results. **G:** Ratio total

number of adipocytes/total number of cells (estimated by nuclei staining). For each biopsy, the number of perilipin-positive adipocytes and of the DAPI-positive nuclei was counted in 5 random microscopic fields; the dots indicate the average ratios for each biopsy. Bars represent the mean from four independent control individuals and three independent lipin-1 defective patients. Student's *t*-test and the Mann-Whitney test were used for controls versus lipin-1 deficient samples comparison. ns, not significant.

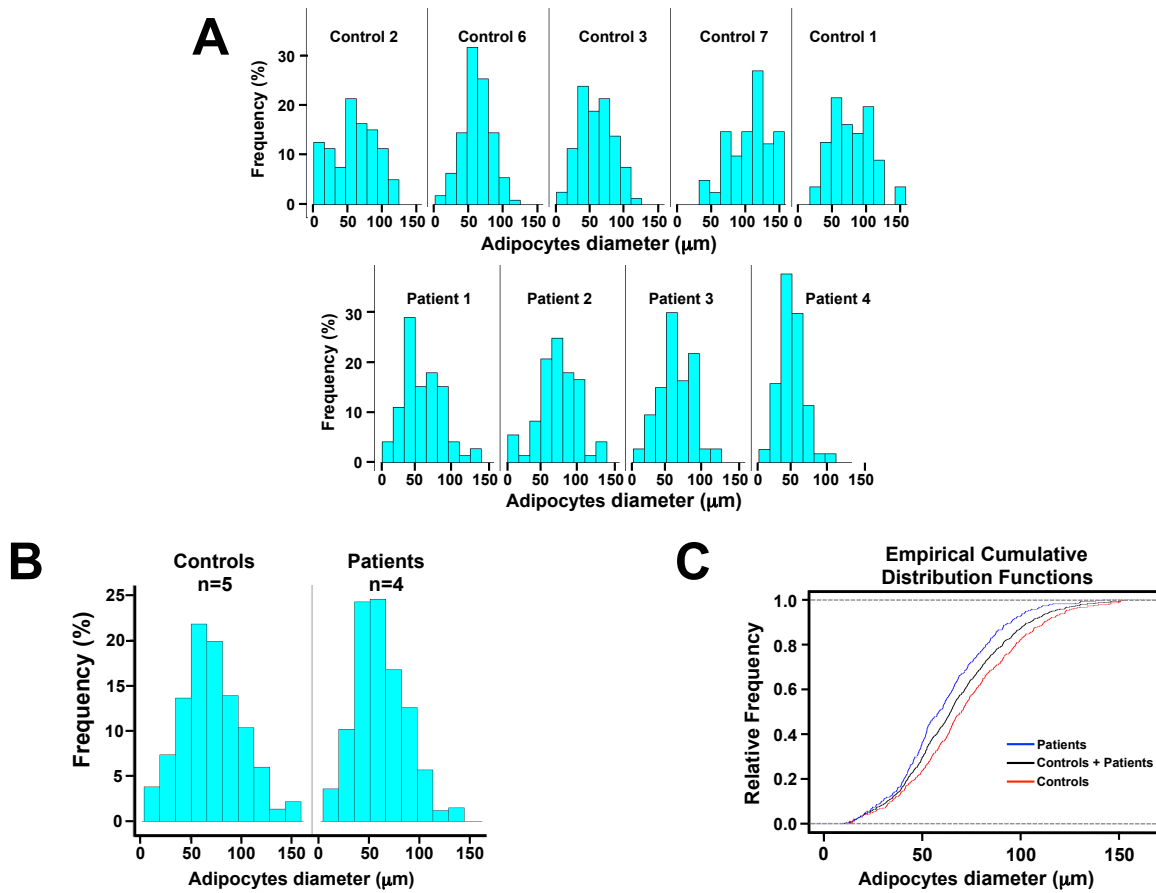


Figure 3. Histomorphometric analysis of the adipocytes diameters in patients carrying biallelic *LPIN1* inactivating mutations. The diameter (expressed in μm) of about 100 adipocytes was measured in each subcutaneous adipose tissue histological section, from 5 normal controls and 4 lipin-1 deficient patients. Control 1, age 12; Control 2, age 15; Control 3, age 18; Control 6, age 15; Control 7, age 15; Patient 1, age 5; Patient 2, age 5; Patient 3, age 11; Patient 4, age 47 (see Table 1). The controls were highly homogeneous in age (controls: $n=5$, mean age: 15; s.d. = 1.9), and treated as a group. Two different statistical approaches were used to minimize the possible confounding effect of age on the adipocytes size (see Results section and Table 2). **A:** histograms of the frequency distribution of the adipocytes diameter for each control and each patient. **B:** histogram of the frequency distribution of the adipocytes diameter for the entire group of controls ($n=5$) and the entire group of patients ($n=4$). **C:** empirical cumulative distribution functions (ECDF) of the adipocytes diameters, for the entire group of 5 controls (red), the entire group of patients (blue), and the whole sample

(controls + patients) (black). These experiments (see Results section and the accompanying Table 2) show a significant decrease in the adipocyte size in the patients compared with normal controls.

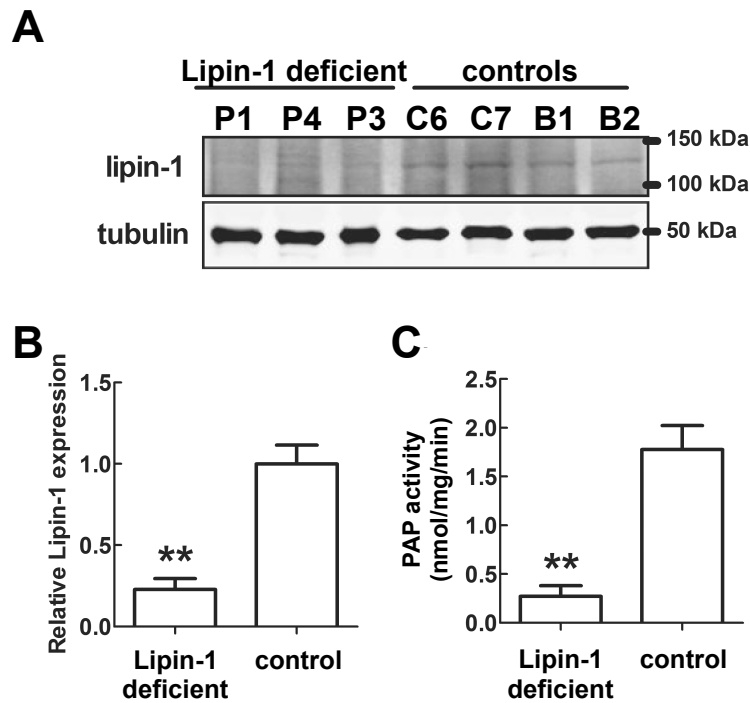


Figure 4. Lipin-1 protein levels and PAP activity in adipose tissue in patients carrying biallelic *LPIN1* inactivating mutations. **A:** Western blotting analysis of lipin-1 protein levels. 60 μ g of total protein extracts from adipose tissue biopsies from three patients and from four normal controls were subjected to WB analysis, with the indicated specific antibodies. Two samples of breast adipose tissue (B1 and B2) were also used as controls, due to paucity of the biopsied subcutaneous WAT controls. Legend: **P1** and **P4**: subcutaneous WAT from Patient 1 and Patient 4 (see Table 1), carrying the *LPIN1* homozygous early stop mutations p.Arg388X/p.Arg388X; **P3**, subcutaneous WAT from Patient 3 (see Table 1) carrying the *LPIN1* heterozygous mutations p.Asn417LysfsX22/p.Glu766_Ser838del (i.e. an early stop mutation and a C-terminal deletion); **C6** and **C7**, subcutaneous WAT from normal individuals (Control 6 and Control 7, see Table 1); **B1** and **B2**: control WAT from adult breast, obtained from two normal individuals, respectively 53 and 56 years old, subjected to reduction mastoplasty (see Methods). **B:** Densitometric analysis of the relative lipin-1 protein levels, equalized

for tubulin expression; protein levels were obtained from the WB in (A), and shown as means \pm S.D. of three (patients) or of four (controls) independent determinations. C: PAP activity for the same samples shown in (A). The values in panels B and C for the controls adipose tissue showed that that both measures were tightly grouped for the subcutaneous WAT controls (C6 and C7) and for the breast WAT controls (B1 and B2), and did not depend on the anatomical location of the biopsied samples. In B and C significant differences are indicated by **, $P < 0.01$ (Student's *t*-test).

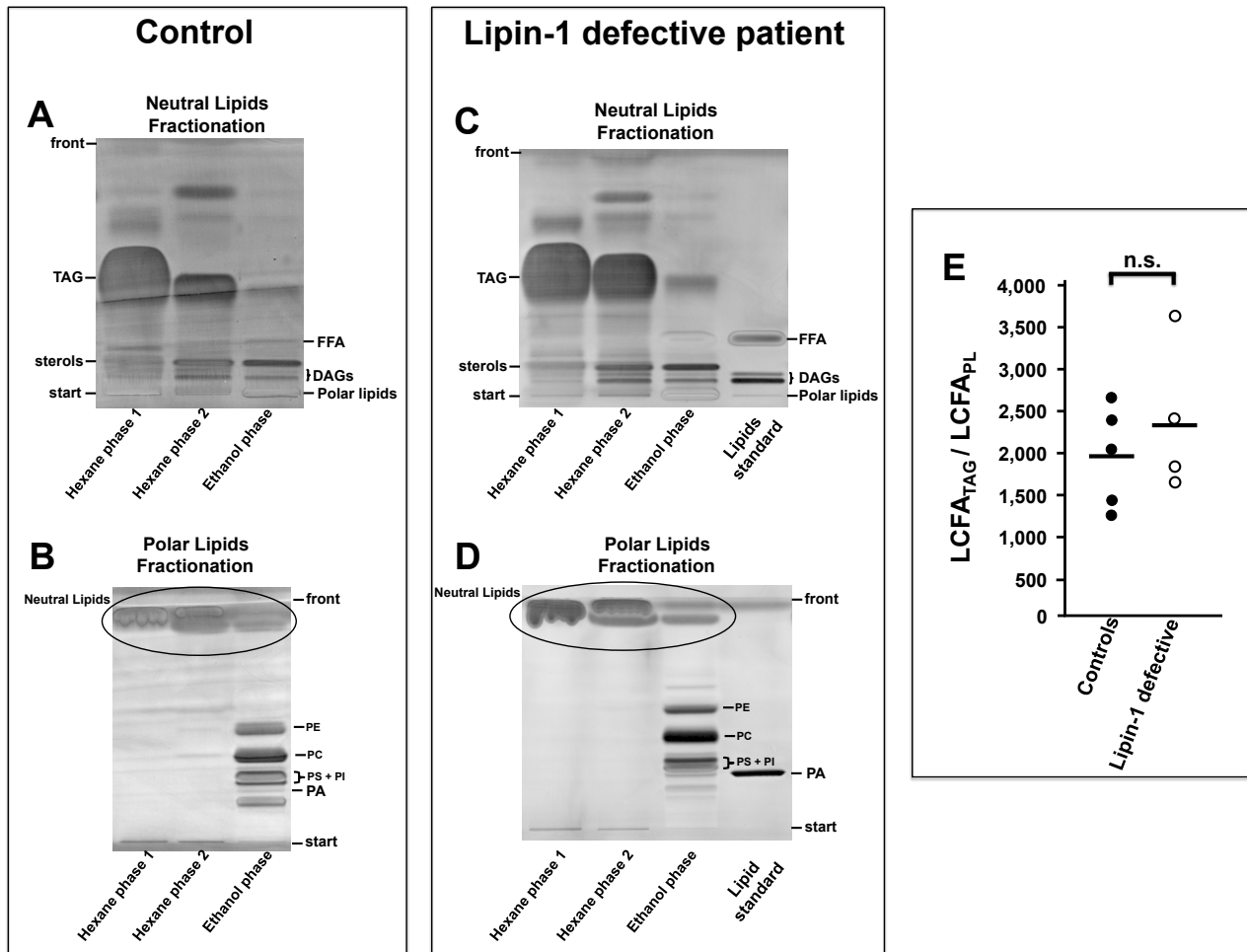


Figure 5. Qualitative lipid analysis of adipose tissue from lipin-1 defective patients and normal controls. **A-D:** representative high performance TLC of the hexane and the ethanol total lipid extraction fractions (35) obtained from subcutaneous WAT biopsies from a normal control individual (A and B) and from a lipin-1 defective patient (C and D). Similar experiments were repeated using adipose biopsies from five control individuals and from four independent lipin-1 defective patients, obtaining analogous results. **A and C:** neutral lipids TLC separation. **B and D:** polar lipids (PL) TLC separation. Legend TAG: triacylglycerols; FFA: unesterified (free) fatty acids; DAG: diacylglycerol; PE: phosphatidylethanolamine; PC: phosphatidylcholine; PS: phosphatidylserine; PI: phosphatidylinositol; PA: phosphatidate. As shown in A and C, the hexane extraction phases: i) contained the whole TAG, ii) contained a part of sterols and DAG, iii) presented negligible amounts of unesterified FA, and iv) were devoid of PL. As shown in B and D, the ethanol extraction phases: i) contained the whole TAG, ii) contained a part of sterols and DAG, iii) presented negligible amounts of unesterified FA, and iv) were devoid of PL.

contained the totality of PL; ii) contained the remaining part of sterols, and iii) presented only traces of TAG, and negligible amounts of unesterified FA. **E:** ratio $LCFA_{TAG}/LCFA_{PL}$. The relative abundance of TAG and PL in the total lipid extracts from each biopsy, was determined by the internal ratio $LCFA_{TAG}/LCFA_{PL}$, corresponding, to the mass in μg of long-chain fatty acids derived from TAG ($LCFA_{TAG}$) divided for the mass in μg of LCFA derived from whole polar lipids PL ($LCFA_{PL}$). The silica gel zones of in the TLC corresponding to TAG and PL were scrapped from the respective TLC plate, and the lipids analyzed by gas-chromatography (GC-FID). Bars represent the means of the ratios $LCFA_{TAG}/LCFA_{PL}$ from five independent control individuals (mean = 1,959) and from four independent lipin-1 defective patients (mean = 2,355). Student's *t*-test was used for controls versus lipin-1 deficient comparison. ns, not significant.

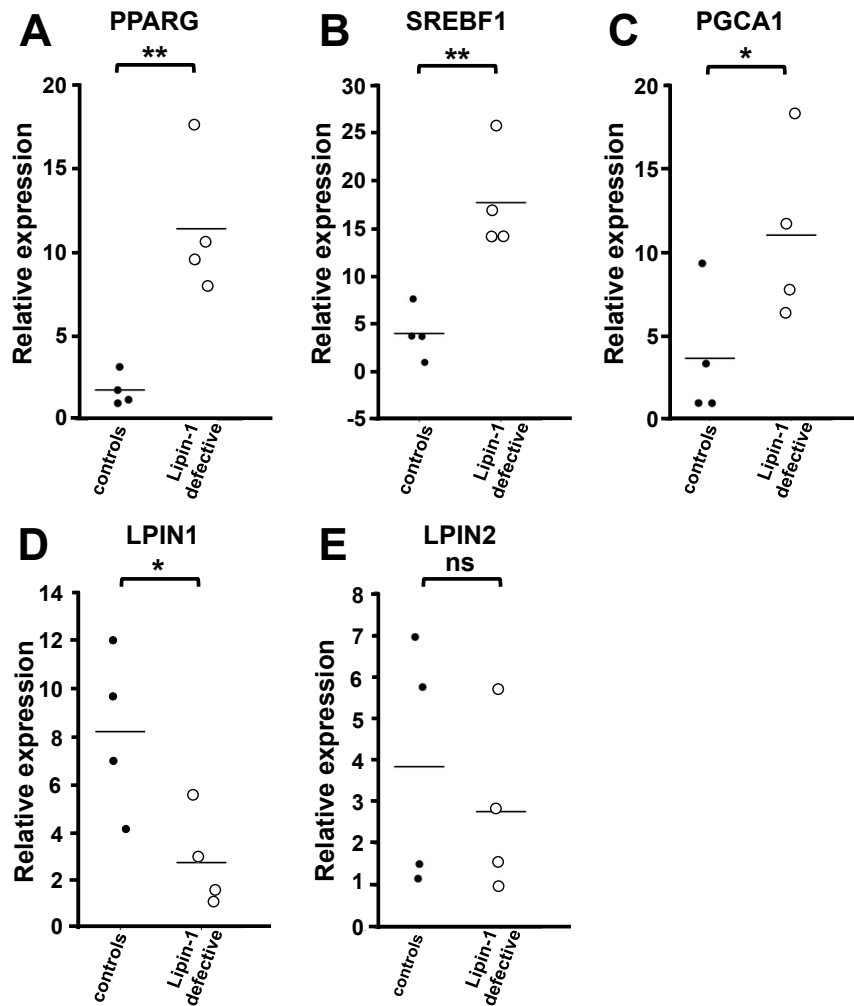


Figure 6. Expression analysis of key adipogenic genes in fat biopsies from lipin-1 defective patients.

Subcutaneous adipose tissue biopsies from four independent lipin-1 defective patients and four independent control (healthy) individuals were collected and total RNA extracted. First-strand cDNA was generated from 1 μ g of total RNA, to perform real-time PCR using specific primers for *PPARG*, *SREBF1*, *PGCA1*, *LPIN1*, *LPIN2* and *ACTB*. Expression data were normalized using *ACTB* as housekeeping gene. Relative expression values are expressed as mean values (bars). ns, not significant; *, $P < 0.05$; **, $P < 0.01$ (Student's *t*-test).

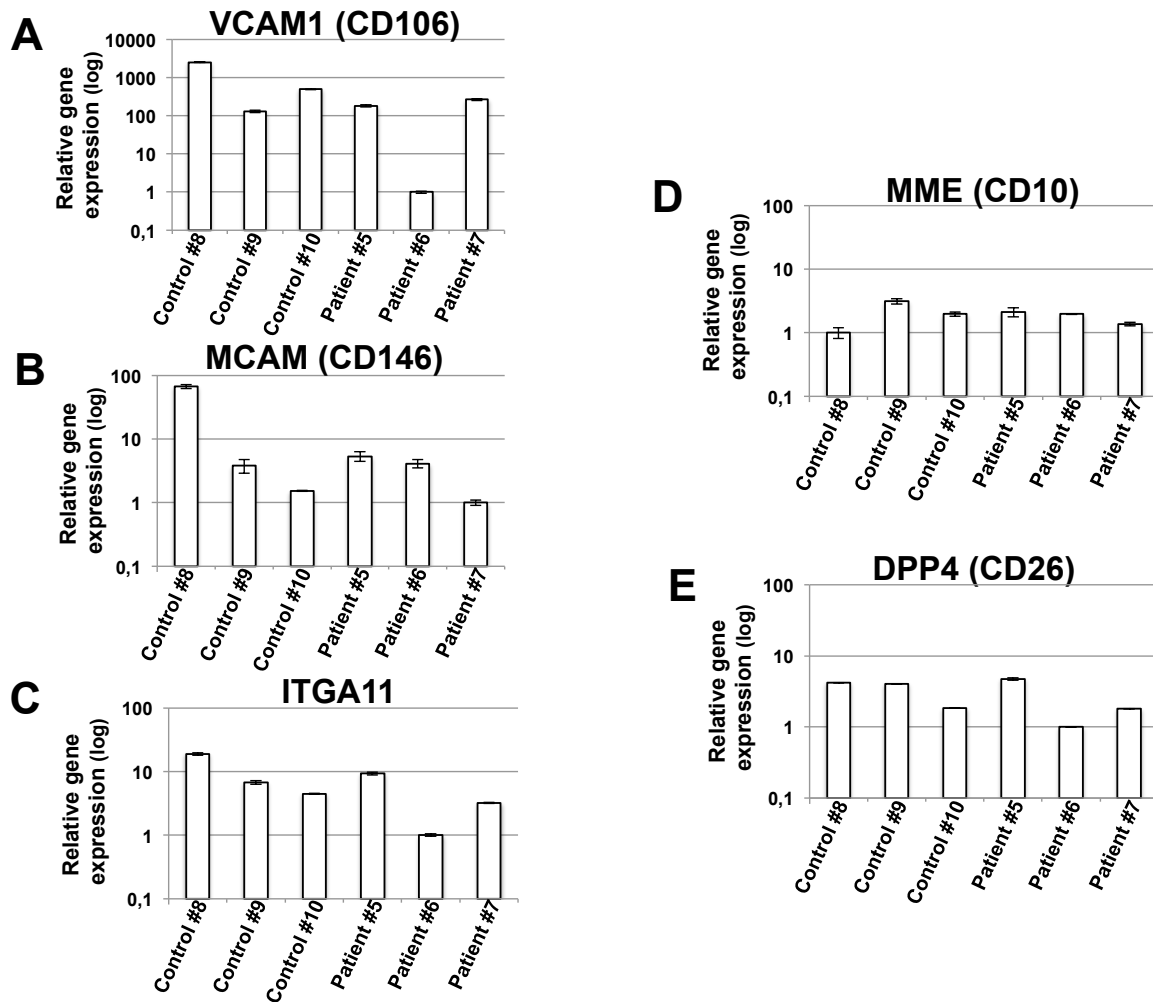


Figure 7. Human dermal primary fibroblasts populations derived from patients carrying biallelic *LPIN1* inactivating mutations or from control individuals express MSC-specific cell surface markers. Human dermal primary fibroblasts populations derived from normal control (healthy) individuals or from lipin-1 defective patients (Table 1) were cultured until confluence in GM. After one day of confluence, cells were harvested, total RNA extracted and first-strand cDNA generated from 1 μ g of total RNA, to perform real-time PCR using specific primers for *VCAM-1* (CD106), *MCAM* (CD146), *ITGA11*, *MME* (CD10) and *DPP4* (CD26). Expression data were normalized using *ACTB* as housekeeping gene. Relative expression values are expressed as means values \pm SD, and shown in logarithmic scale.

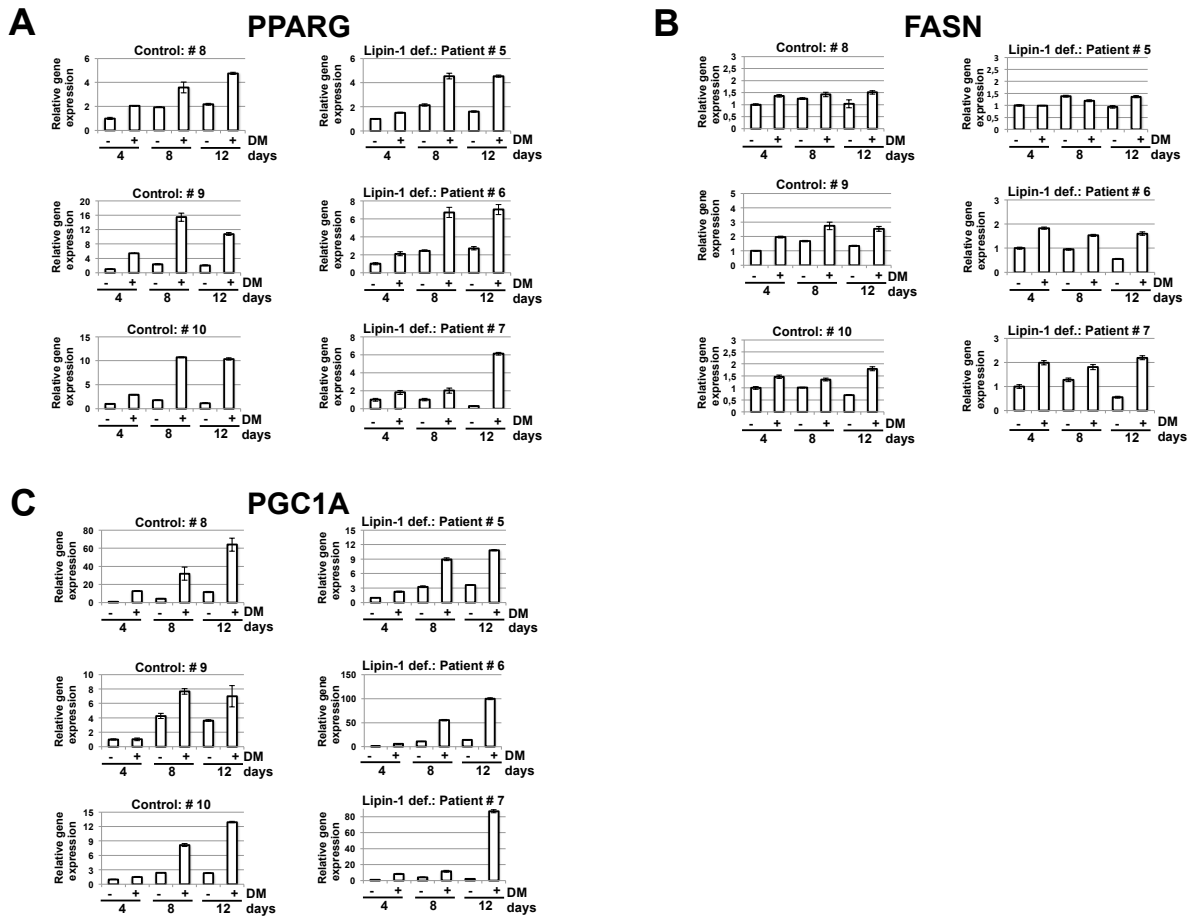


Figure 8. Human fibroblasts populations derived from patients carrying biallelic *LPIN1* inactivating mutations can be induced to adipogenic differentiation. Human dermal primary fibroblasts populations derived from normal control (healthy) individuals or from lipin-1 defective patients (see Table 1) were cultured until confluence in GM. Cells were then shifted to adipogenic differentiation medium, DM (+), containing insulin, DXM, IBMX and indometacin, or left in GM (-). After 4, 8 or 12 days in DM cells were harvested, the total RNA extracted and the first-strand cDNA generated from 1 µg of total RNA, to perform real-time PCR using specific primers for *PPARG*, *FASN* and *PGC1A*. Expression data were normalized using actin beta (*ACTB*) as housekeeping gene. Relative expression ± SD is shown in the histograms.